Quantum Optics in Cavities, Phase Space Representations, and the Classical Limit of Quantum Mechanics*

Luiz Davidovich
Instituto de Física, Universidade Federal do Rio de Janeiro
Cx. P. 68528, 21945-970 Rio de Janeiro, Rio de Janeiro, Brazil

These lectures review some basic techniques of quantum optics, related to the description of the quantized electromagnetic field in phase space and of the interaction between atoms and photons in cavities. The Wigner function is introduced, and some of the methods for measuring this distribution are reviewed. The combination of phase space methods with cavity QED techniques is shown to lead to experiments which are closely connected to fundamental problems regarding the classical limit of quantum mechanics and the quantum theory of measurement.

Contents

*Lecture notes for the Pan American Advanced Study Institute on "Chaos, decoherence and quantum entanglement," Ushuaia, Argentina, October 2000.

I. INTRODUCTION

One of the most subtle problems in the physics of this century is the relation between the macroscopic world, described by classical physics, and the microscopic world, ruled by the laws of quantum physics. Among the several questions involved in the quantum-classical transition, one stands out in a striking way. As pointed out by Einstein in a letter to Max Born in 1954 [1], it concerns "the inexistence at the classical level of the majority of states allowed by quantum mechanics," namely coherent superpositions of classically distinct states. Indeed, while in the quantum world one frequently comes across coherent superpositions of states (like in Young's two-slit interference experiment, in which each photon is considered to be in a coherent superposition of two wave packets, centered around the classical paths which stem out of each slit), one does not see macroscopic objects in coherent superpositions of two distinct classical states, like a stone which could be at two places at the same time. There is an important difference between a state of this kind and one which would involve just a classical alternative: the existence of quantum coherence between the two localized states would allow in principle the realization of an interference experiment, complementary to the simple observation of the position of the stone. We know all this already from Young's experiment: the observation of the photon path (that is, a measurement which is able to distinguish through which slit the photon has passed) unavoidably destroys the interference fringes.

If one assumes that the usual rules of quantum dynamics are valid up to the macroscopic level, then the existence of quantum interference at the microscopic level necessarily implies that the same phenomenon should occur between distinguishable macroscopic states. This was emphasized by Schrödinger in his famous "cat paradox" [2]. An important role is played by this fact also in quantum measurement theory, as pointed out by Von Neumann [3]. Indeed, let us assume for instance that a microscopic two-level system (states $|+\rangle$ and $|-\rangle$) interacts with a macroscopic measuring apparatus, in such a way that the pointer of the apparatus points to a different (and classically distinguishable!) position for each of the two states, that is, the interaction transforms the joint atom-apparatus initial state into

$$|+\rangle|\uparrow\rangle \rightarrow |+\rangle'|\nearrow\rangle\,,$$
$$|-\rangle|\uparrow\rangle \rightarrow |-\rangle'|\nwarrow\rangle\,.$$

The linearity of quantum mechanics implies that, if the quantum system is prepared in a coherent superposition of the two states, say $|\psi\rangle = (|+\rangle + |-\rangle)/\sqrt{2}$, the final state of the complete system should be a coherent superposition of two correlated states, each of which corresponding to a different position of the pointer:

$$\begin{aligned}&(1/\sqrt{2})(|+\rangle + |-\rangle)|\uparrow\rangle \\ &\rightarrow (1/\sqrt{2})(|+\rangle'|\nearrow\rangle + |-\rangle'|\nwarrow\rangle) = (1/\sqrt{2})(|\nearrow\rangle' + |\nwarrow\rangle')\,,\end{aligned} \tag{1}$$

where in the last step it was assumed that the two-level system is incorporated into the measurement apparatus after their interaction (for instance, an atom which gets stuck to the detector). One gets, therefore, as a result of the interaction between the microscopic and the macroscopic system, a coherent superposition of two classically distinct states of the macroscopic apparatus. This is actually the situation in Schrödinger's cat paradox: the cat can be viewed as a measuring apparatus of the state of a decaying atom, the state of life or death of the cat being equivalent to the two positions of the pointer. This would imply that one should be able in principle to get interference between the two states of the pointer: it is precisely the lack of evidence of such phenomena in the macroscopic world which motivated Einstein's concern.

Faced with this problem, Von Neumann introduced through his collapse postulate [3] two distinct types of evolution in quantum mechanics: the deterministic and unitary evolution associated to the Schrödinger equation, which describes the establishment of a correlation between states of the microscopic system being measured and distinguishable classical states (for instance, distinct positions of a pointer) of the macroscopic measurement apparatus; and the probabilistic and irreversible process associated with measurement, which transforms the correlated state into a statistical mixture. This separation of the whole process into two steps has been the object of much debate [4–6]; indeed, it would not only imply an intrinsic limitation of quantum mechanics to deal with classical objects, but it would also pose the problem of drawing the line between the microscopic and the macroscopic world.

Several possibilities have been explored as solutions to this paradox, including the proposal that a small non-linear term in the Schrödinger equation, although unnoticeable for microscopic phenomena, could eliminate the coherence between macroscopic states, thus transforming the quantum superpositions into statistical mixtures [4]. The non-observability of the coherence between the two positions of the pointer has been attributed both to the lack of non-local observables with matrix elements between the two corresponding states [7] as well as to the fast decoherence due to dissipation [8–10]. This last approach has been emphasized in recent years: decoherence follows from the irreversible coupling of the observed system to a reservoir [8,9]. In this process, the quantum superposition is turned into a statistical mixture, for which all the information on the system can be described in classical terms, so our usual perception of the world is recovered. Furthermore, for macroscopic superpositions quantum coherence decays much faster than the physical observables of the system, its decay time being given by the dissipation time divided by a dimensionless number measuring the "separation" between the two parts. The statement that these two parts are macroscopically separated implies that this separation is an extremely large number. Such is the case for biological systems like "cats" made of huge number of molecules. In the simple case mentioned by Einstein [1], of a particle split into two spatially separated wave packets by a distance d, the dimensionless measure of the separation is $(d/\lambda_{dB})^2$, where λ_{dB} is the particle de Broglie wavelength. For a particle with mass equal to 1 g at a temperature of 300 K, and $d = 1$ cm, this number is about 10^{40}, and the decoherence is for all purposes instantaneous. This would provide an answer to Einstein's concern: decoherence of macroscopic states would be too fast to be observed.

In these lectures, it will be shown that the study of the interaction between atoms and electromagnetic fields in cavities can help us understand some aspects of this problem. In fact, many recent contributions in the field of quantum optics have led not only to the investigation of the subtle frontier between the quantum and the classical world, but also of hitherto unsuspected quantum mechanical processes like teleportation [11]. Research on quantum optics is therefore intimately entangled with fundamental problems of quantum mechanics.

The whole area of "cavity quantum electrodynamics" is a very recent one. It concerns the interactions between atoms and discrete modes of the electromagnetic field in a cavity, under conditions such that losses due to dissipation and atomic spontaneous emission are very small. Usually, one deals with atomic beams crossing cavities with a high quality factor Q (defined as the product of the angular frequency of the mode and its lifetime, $Q = \omega\tau$). The atoms, prepared in special states and detected after interacting with the field, serve two purposes: they are used to manipulate the field in the cavity, so as to produce the desired states, and also to measure the field.

Several factors contributed to the development of this area. The production of superconducting Niobium cavities, with extremely high quality factors, up to the order of 10^{10}, allows one to keep a photon in the cavity for a time of the order of one second. New techniques of atomic excitation [37] (alkaline atoms, like Rubidium and Cesium, are frequently used for this purpose) to highly excited levels (principal quantum numbers of the order of 50), and with maximum angular momentum ($\ell = n - 1$) – the so-called planetary Rydberg atoms – have led to the production of atomic beams that interact strongly even with very weak fields, of the order of one photon, due to the large magnitude of the relevant electric dipoles. Besides, the lifetime of these states is large – of the order of the millisecond – which may be understood semiclassically, from the correspondence principle (which should be valid for $n \sim 50$): the electron is always very far away from the nucleus, and therefore its acceleration is small, implying weak radiation and a long lifetime. One should also mention the new techniques of atomic velocity control, which allow the production of approximately monokinetic atomic beams, leading to a precise control of the interaction time between atom and field. For a review of some of the main problems and results in this field, see Ref. [13].

Looking into the problem of the classical limit of quantum mechanics will actually provide us with a useful thread, a "leitmotif" which will lead us to many important techniques of quantum optics.

We start these lectures by reviewing some of the basic properties of the quantized electromagnetic field. We introduce then the Wigner function, which allows the complete characterization of the state of the field. Furthermore, this function has been measured in a number of experiments. We discuss then the interaction of two-level atoms with the quantized electromagnetic field, and recover in the proper limit semiclassical equations of motion for the atom. We discuss then some experiments which have tested basic models of quantum optics, regarding the interaction between atoms and fields in cavities.

II. THE QUANTIZED ELECTROMAGNETIC FIELD

The free-field Hamiltonian for a mode of the electromagnetic field is given by the harmonic oscillator expression

$$\hat{H} = \hbar\omega \left(\hat{N} + \tfrac{1}{2}\right) , \tag{2}$$

where $\hat{N} = \hat{a}^\dagger \hat{a}$ is the *number operator*, and $\hat{a}$ and $\hat{a}^\dagger$ satisfy the commutation relation

$$[\hat{a}, \hat{a}^\dagger] = 1\,. \tag{3}$$

The eigenstates of $\hat{H}$ are denoted by $|n\rangle$, and satisfy the equation

$$\hat{N}|n\rangle = n|n\rangle\,, \tag{4}$$

while the eigenenergies are given by $E_n = (n + 1/2)\hbar\omega$. It is easy to show that

$$\hat{a}^\dagger|n\rangle = \sqrt{n+1}|n+1\rangle\,,\ \hat{a}|n\rangle = \sqrt{n}|n-1\rangle\,. \tag{5}$$

The eigenvalue n of the number operator $\hat{N}$ is interpreted as the number of photons in the field, while, in view of (5), $\hat{a}$ and $\hat{a}^\dagger$ are the photon *annihilation* and *creation* operators.

The states $|n\rangle$ are the so-called *Fock states*, and have a well-defined number of photons. The state corresponding to $n = 0$ is the *vacuum state*. It is easy to show from the above relations that

$$|n\rangle = \frac{\hat{a}^{\dagger n}}{\sqrt{n!}}|0\rangle\,.$$

The electric field is expressed in terms of the annihilation and creation operators by

$$\vec{E}(r) = E_\omega[\hat{a}u(\vec{r})\,\vec{\epsilon} + \hat{a}^\dagger u^*(\vec{r})\,\vec{\epsilon}^{\,*}]\,, \tag{6}$$

where $u(\vec{r})$ is a function which describes the spatial dependence of the field mode, $\vec{\epsilon}$ is the polarization vector, and $E_w = \sqrt{h\omega/V}$ is the *field per photon*. Here $V = \int |u(\vec{r})|^2 d^3r$ is the effective volume of the mode, defined so that the expectation value of the electromagnetic energy in the vacuum state, $(1/4\pi)\int\langle 0|[\vec{E}(\vec{r})]^2|0\rangle d^3r$, is equal to the zero-point energy $\hbar\omega/2$. One should note that $\langle n|\hat{E}|n\rangle = 0$, that is, the average electric field is zero in a Fock state.

A special role will be played in the following by the *phase displacement operator*:

$$\hat{U}(\theta) = \exp(-i\theta\hat{N})\,. \tag{7}$$

It follows from the commutation relations that

$$\hat{U}^\dagger(\theta)\hat{a}\hat{U}(\theta) = \hat{a}\exp(-i\theta)\,. \tag{8}$$

For $\theta = \omega t$, the phase displacement operator coincides, up to a factor $\exp(-i\omega t/2)$ coming from the zero-point energy, with the evolution operator corresponding to the Hamiltonian (2), and (8) yields the time evolution of the Heisenberg operator associated with $\hat{a}$.

A. Quadratures of the electromagnetic field

The quadratures of the electromagnetic field correspond to the position and momentum of a harmonic oscillator:

$$\hat{q} = \frac{1}{\sqrt{2}}\left(\hat{a} + \hat{a}^\dagger\right), \quad \hat{p} = \frac{i}{\sqrt{2}}\left(\hat{a}^\dagger - \hat{a}\right), \quad [\hat{q}, \hat{p}] = i\,. \tag{9}$$

This commutation relation implies the Heisenberg inequality $\Delta q\Delta p \geq 1/2$.

¿From (8) and (9), we see that, for $\theta = \pi$,

$$\hat{U}^\dagger(\pi)\hat{q}\hat{U}(\pi) = -\hat{q}\,, \qquad \hat{U}^\dagger(\pi)\hat{p}\hat{U}(\pi) = -\hat{p}\,,$$

so that $\hat{U}(\pi)$ is the *parity operator*.

Setting $u(\vec{r}) = |u(\vec{r})|\exp[-i\phi(\vec{r})]$ in Eq. (6), we have, in the Heisenberg picture, for the electric field operator in terms of these quadratures (for a real polarization vector):

$$\vec{E}(r,t) = E_\omega|u(\vec{r})|\sqrt{2}[\hat{q}\cos(\omega t + \phi) - \hat{p}\sin(\omega t + \phi)]\,\vec{\epsilon}\,.$$

This expression is analogous to the one which yields the position of a harmonic oscillator at time t in terms of its initial position and momentum:

$$x(t) = x(t_0)\cos\omega(t-t_0) + \frac{p(t_0)}{m\omega}\sin\omega(t-t_0)\,. \tag{10}$$

The quadrature eigenstates (which correspond to states with well-defined position and momentum for the harmonic oscillator) will be denoted by

$$\hat{q}|q\rangle = q|q\rangle\,, \qquad \hat{p}|p\rangle = p|p\rangle\,.$$

As for the position and momentum eigenstates, these states provide two non-normalizable bases. The corresponding quadrature wave functions are given by

$$\psi(q) = \langle q|\psi\rangle\,,\ \tilde{\psi}(p) = \langle p|\tilde{\psi}\rangle\,.$$

Using the phase displacement operator given by (7), it is possible to define *generalized quadratures*:

$$\hat{q}_\theta = \hat{U}^\dagger(\theta)\hat{q}\,\hat{U}(\theta) = (1/\sqrt{2})\left(\hat{a}e^{-i\theta} + \hat{a}^\dagger e^{i\theta}\right) = \hat{q}\cos\theta + \hat{p}\,\sin\,\theta\,, \tag{11}$$

$$\hat{p}_\theta = \hat{U}^\dagger(\theta)\hat{p}\,\hat{U}(\theta) = -\hat{q}\sin\theta + \hat{p}\,\cos\,\theta\,. \tag{12}$$

It is clear from these expressions that $\hat{U}(\theta)$ is the rotation operator in phase space. For a harmonic oscillator, and with $\theta = \omega t$, (11) and (12) correspond respectively to the position and the momentum of the oscillator at time t, expressed in terms of the position $\hat{q}$ and momentum $\hat{p}$ at time $t = 0$.

B. Coherent states

We have seen that the average value of the electric field operator vanishes in a Fock state. Therefore, we cannot associate Fock states to classical fields with amplitude different from zero, and well-defined phase. Let us look now for "quasi-classical" field states. We require that the average value of the electromagnetic field in these states, which we denote by $|\alpha\rangle$, coincides with the classical expression for an electromagnetic field with complex amplitude α:

$$\langle\alpha|\vec{E}(\vec{r})|\alpha\rangle = \sqrt{\hbar\omega/V}u(\vec{r})\vec{\epsilon}\,\alpha + c.c.\,. \tag{13}$$

¿From (6) and (13) it follows that

$$\langle\alpha|\hat{a}|\alpha\rangle = \alpha\,. \tag{14}$$

We also require that the expectation value of the electromagnetic energy in the state $|\alpha\rangle$ coincides with the classical expression for this energy, expressed in terms of the complex amplitude α, at least in the limit when $|\alpha| \gg 1$. It is easy to show that the classical energy, when the electric field is expressed in terms of α like in (13), is given by $E_{\rm cl} = \hbar\omega|\alpha|^2$. Comparing this expression with (2), we must have therefore

$$\langle\alpha|\hat{a}^\dagger\hat{a}|\alpha\rangle = |\alpha|^2\,. \tag{15}$$

¿From (14) and (15) it follows that

$$\langle\alpha|(\hat{a}^\dagger - \alpha^*)(\hat{a} - \alpha)|\alpha\rangle = 0\,, \tag{16}$$

and therefore the state $|\alpha\rangle$ must be an eigenstate of the annihilation operator $\hat{a}$ with eigenvalue α:

$$\hat{a}|\alpha\rangle = \alpha|\alpha\rangle. \tag{17}$$

These are the *coherent states* [14], which play an important role in quantum optics, and also in the understanding of the classical limit of quantum mechanics.

It is clear from the above discussion that the average number of photons in a coherent state $|\alpha\rangle$ is given by

$$\langle n\rangle = \langle\alpha|\hat{a}^\dagger\hat{a}|\alpha\rangle = |\alpha|^2\,.$$

It also follows from the definition (17) and the commutation relations that, for a coherent state,

$$\Delta q = \Delta p = 1/\sqrt{2}\,,$$

or, more generally, $\Delta q_\theta = 1/2$. Therefore, coherent states are minimum uncertainty states. This property can be pictorially depicted by drawing in phase space a circle, with a radius equal to the uncertainty in Δq or Δp, as shown in Fig. 1

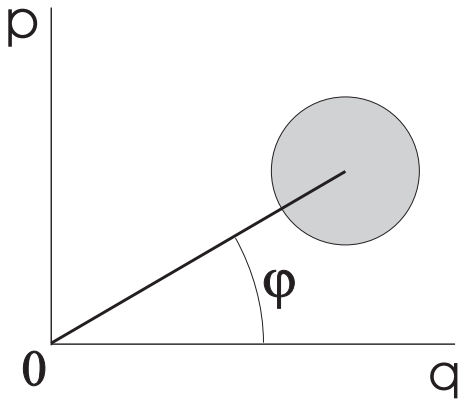

FIG. 1. Pictorial representation of a coherent state in phase space.

In terms of Fock states, coherent states can be expressed in the following way:

$$\mid \alpha\rangle = e^{-|\alpha|^2/2} \sum_{n=0}^{\infty} \frac{\alpha^n}{\sqrt{n!}} \mid n\rangle = e^{-|\alpha|^2/2} \sum_{n=0}^{\infty} \frac{(\alpha \hat{a}^\dagger)^n}{n!} \mid 0\rangle \,, \tag{18}$$

corresponding to the photon number distribution

$$p(n) = \mid \langle n \mid \alpha \rangle \mid^2 = \exp(- \mid \alpha \mid^2) \frac{\mid \alpha \mid^{2n}}{n!} = \exp(-\langle n \rangle) \frac{\langle n \rangle^n}{n!} \,. \tag{19}$$

This is a Poisson distribution, with the variance $(\Delta n)^2 = \langle n \rangle$.

The *displacement operator* is defined by

$$\hat{D}(\alpha, \alpha^*) = \exp\left(\alpha \hat{a}^\dagger - \alpha^* \hat{a}\right) \,. \tag{20}$$

Note that the right-hand side of (18) implies that

$$|\alpha\rangle = e^{-|\alpha|^2/2} e^{\alpha \hat{a}^\dagger} |0\rangle = e^{-|\alpha|^2/2} e^{\alpha \hat{a}^\dagger} e^{-\alpha \hat{a}} |0\rangle = \exp\left(\alpha \hat{a}^\dagger - \alpha^* \hat{a}\right) |0\rangle = \hat{D}(\alpha, \alpha^*) |0\rangle \,, \tag{21}$$

where in the last step the Baker-Hausdorff transformation has been used to entangle the annihilation and creation operators in the exponent. Therefore, a coherent state $|\alpha\rangle$ can be obtained by applying the displacement operator $\hat{D}(\alpha, \alpha^*)$ to the vacuum state. The displacement operator is closely connected to the evolution operator corresponding to the interaction of the electromagnetic field with a classical current. Indeed, this interaction is described by the Hamiltonian

$$H_{\rm int} = \int \vec{J} \cdot \vec{A} \, d^3 r \,,$$

which can be written in the form $H_{\rm int} = i(\alpha \hat{a}^\dagger - \alpha^* \hat{a})$. The evolution operator corresponding to this interaction coincides, up to a phase, with $D(\alpha, \alpha^*)$. Therefore, Eq. (21) implies that classical currents generate coherent states from the vacuum.

¿From the expansion of the coherent states in terms of the Fock states, one easily derives the following orthonormality and completeness relations:

$$\mid \langle \alpha \mid \alpha' \rangle \mid^2 = e^{-|\alpha - \alpha'|^2} \,,$$

$$\frac{1}{\pi} \int d^2\alpha \mid \alpha \rangle \langle \alpha \mid = \mathcal{I} \,,$$

where $d^2\alpha \equiv d(\Re e\alpha)d(\Im m\alpha)$.

In terms of the quadrature eigenstates $|q\rangle$, one may write:

$$\langle q|\alpha_0\rangle = (1/\pi)^{1/4} e^{-iq_0p_0/2} e^{ip_0q} e^{-(q-q_0)^2/2}\,,$$

with $\alpha_0 = (q_0 + ip_0)/\sqrt{2}$.

Therefore, the probability of finding a quadrature $\hat{q}$ of the field with a value q, for a coherent state $|\alpha_0\rangle$, is given by a Gaussian (for the vacuum, $q_0 = p_0 = 0$):

$$P(q) = (1/\pi)^{1/2} \exp[-(q-q_0)^2]\,.$$

C. Squeezed states

The most general family of minimum uncertainty states, as shown by Pauli [15], corresponds to the following wave function in the q-quadrature representation:

$$\psi(q) = \langle q|\psi\rangle = (2\pi\Delta^2 q)^{-1/4} \exp(ip_0q) \exp\left(\frac{-(q-q_0)^2}{4\Delta^2 q}\right).$$

The variance $\Delta^2 q$ is not necessarily equal to $1/2$, as it is for coherent states. In the q_θ-representation, one would get the same expression for $\psi(q_\theta)$, with q, q_0, p_0, and $\Delta^2 q$ replaced by q_θ, $q_{\theta 0}$, $p_{\theta 0} = q_{\theta+\pi/2,0}$, and $\Delta^2 q_\theta$, respectively. If $\Delta^2 q_\theta < 1/2$ for some region of values of θ, we say that the state is squeezed.

It is clear that this family of minimum uncertainty squeezed states can be obtained from coherent states through a scale transformation, which compresses say the q-axis and at the same time dilates the p-axis. Thus, the wave function of the squeezed vacuum would be obtained from the one corresponding to a coherent state by the scale transformation [16]:

$$\phi_0(q,\xi) = e^{\xi/2}\psi_0\left(e^{\xi}q\right)\,, \qquad \tilde{\phi}_0(p,\xi) = e^{-\xi/2}\tilde{\psi}_0\left(e^{-\xi}p\right)\,,$$

where

$$\psi_0(q) = (1/\pi)^{1/4} e^{-q^2/2}\,.$$

Differentiating $\phi_0(q,\xi) = \langle q|\phi_0(\xi)\rangle$ with respect to ξ, one gets:

$$\begin{aligned}\frac{\partial}{\partial\xi}\langle q|\phi_0(\xi)\rangle = \frac{\partial}{\partial\xi}\phi_0(q,\xi) &= \frac{1}{2}\phi_0 + q\frac{\partial\phi_0}{\partial q} = \frac{1}{2}\left(q\frac{\partial}{\partial q} + \frac{\partial}{\partial q}q\right)\phi_0 \\ &= \frac{i}{2}\langle q|(\hat{q}\hat{p} + \hat{p}\hat{q})|\phi_0(\xi)\rangle\,. \end{aligned} \tag{22}$$

Therefore,

$$\frac{\partial}{\partial\xi}|\phi_0(\xi)\rangle = \frac{i}{2}(\hat{q}\hat{p} + \hat{p}\hat{q})|\phi_0(\xi)\rangle = \frac{1}{2}\left(\hat{a}^2 - \hat{a}^{\dagger 2}\right)|\phi_0(\xi)\rangle\,,$$

and

$$|0,\xi\rangle = \hat{S}(\xi)|0\rangle\,,$$

where $\hat{S}(\xi) = \exp\left[(\xi/2)\left(\hat{a}^2 - \hat{a}^{\dagger 2}\right)\right]$ is the *squeezing operator*.

More generally, one could set $\xi = re^{i\theta}$, implying a combination of squeezing and rotation, which would correspond to compressing the quadrature $q_{\theta/2}$ and dilating the quadrature $q_{\theta/2+\pi/2}$.

A more general family of minimum uncertainty squeezed states is obtained by displacing the squeezed vacuum, with the displacement operators introduced before:

$$|\alpha,\xi\rangle = \hat{D}(\alpha)\hat{S}(\xi)|0\rangle\,. \tag{23}$$

An equivalent result is obtained by applying the squeezing transformation to the coherent state $|\alpha\rangle$.

One should note that the squeezing operator can be interpreted as the evolution operator corresponding to the Hamiltonian

$$H_{\rm int} \propto \hat{a}^2 - \hat{a}^{\dagger 2}\,.$$

Hamiltonians of this form occur in non-linear optics, where they describe degenerate parametric amplifiers. A realization of such an amplifier is provided by a KTP crystal (potassium titanium phosphate) pumped by a laser with frequency twice as large as the mode of interest [17].

The average number of photons in a squeezed state can be immediately obtained from (23):

$$\langle \alpha,\, \xi | a^\dagger a | \alpha,\, \xi \rangle = |\alpha|^2 + \sinh^2 r\,.$$

This equation shows that the average number of photons in the squeezed vacuum is different from zero: energy is required to squeeze the vacuum!

D. Measurement of quadratures

Several methods have been proposed to measure quadratures of the electromagnetic field (for a review, see for instance Ref. [18]). The general idea consists in mixing the signal to be detected with an intense coherent signal, called *local oscillator,* before detection [19].

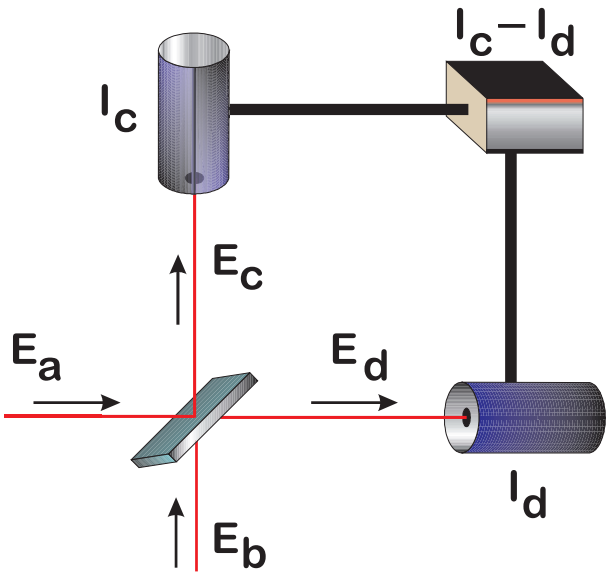

FIG. 2. Method of balanced homodyne detection

The discussion here is restricted to the method of *balanced homodyne detection,* sketched in Fig. 2. The field to be measured (complex amplitude E_a) is sent on a beam splitter, together with a coherent field (complex amplitude E_b) with the same frequency. One measures then the difference of intensity of the two beams emerging from the beam splitter (complex amplitudes E_c and E_d). The detection is said to be balanced when the mirror transmits 50% of the incident light.

Let r and t be the reflection and transmission coefficients of the mirror, respectively. Let us set:

$$E_c = rE_a - tE_b\,, \tag{24a}$$
$$E_d = tE_a + rE_b\,, \tag{24b}$$

or yet, in matrix form,

$$\begin{pmatrix} E_c \\ E_d \end{pmatrix} = \begin{pmatrix} r & -t \\ t & r \end{pmatrix} \begin{pmatrix} E_a \\ E_b \end{pmatrix} . \tag{25}$$

Energy conservation (assuming that losses are negligible) implies that

$$|E_c|^2 + |E_d|^2 = |E_a|^2 + |E_b|^2 . \tag{26}$$

¿From (25) and (26), one gets:

$$|r|^2 + |t|^2 = 1 , \tag{27a}$$
$$r^* t - r t^* = 0 . \tag{27b}$$

If one takes r real and equal to $\sqrt{\eta}$ (one should note that phases in r and t can be removed by redefining the phases of the incoming and outgoing fields), it follows from (27) that $t = \pm(1-\eta)^{1/2}$. Choosing the positive sign, one gets then

$$\begin{pmatrix} E_c \\ E_d \end{pmatrix} = \begin{pmatrix} \sqrt{\eta} & -\sqrt{1-\eta} \\ \sqrt{1-\eta} & \sqrt{\eta} \end{pmatrix} \begin{pmatrix} E_a \\ E_b \end{pmatrix} . \tag{28}$$

Normalizing the intensity to the photon number, and introducing the annihilation operators through

$$E_a \to \hat{a}, \qquad E_b \to \hat{b} ,$$
$$E_c \to \hat{c}, \qquad E_d \to \hat{d} ,$$

one gets, from (28),

$$\hat{c} = \sqrt{\eta}\hat{a} - \sqrt{1-\eta}\,\hat{b} , \qquad \hat{d} = \sqrt{1-\eta}\hat{a} + \sqrt{\eta}\,\hat{b} . \tag{29}$$

For balanced detection, $\eta = 1/2$, so that

$$\hat{c} = \frac{1}{\sqrt{2}}(\hat{a} - \hat{b}) , \qquad \hat{d} = \frac{1}{\sqrt{2}}(\hat{a} + \hat{b}) . \tag{30}$$

Note that conditions (27) imply that the transformation between the field operators corresponding to (25) is unitary (this is the requirement for operators which corresponds to energy conservation for the classical fields).

The difference between the intensities of the fields E_d e E_c is given then by

$$I = \hat{d}^\dagger \hat{d} - \hat{c}^\dagger \hat{c} = \hat{a}^\dagger \hat{b} + \hat{b}^\dagger \hat{a} . \tag{31}$$

Assuming that the field E_b may be described classically (this would be the case for a coherent state with large average photon number), one replaces $\hat{b}$ by $\beta = B\, e^{-i(\omega t - \theta)}$, so that (31) gets transformed into

$$I = B \left[\hat{a} e^{i(\omega t - \theta)} + \hat{a}^\dagger e^{-i(\omega t - \theta)} \right] . \tag{32}$$

Since $\hat{a} = \hat{a}_0 e^{-i\omega t}$ (all fields are taken in the Heisenberg picture), one gets finally,

$$I = B \left(\hat{a}_0\, e^{-i\theta} + \hat{a}_0^\dagger\, e^{i\theta} \right) . \tag{33}$$

This equation shows that the difference of intensities, measured by the method of homodyne detection, is directly proportional to the quadrature $\hat{X}(\theta)$ of the field E_a, defined by

$$\hat{X}(\theta) = \frac{1}{\sqrt{2}} \left(\hat{a}_0 e^{-i\theta} + \hat{a}_0^\dagger e^{i\theta} \right) . \tag{34}$$

Therefore, by detecting the difference of intensities, as the phase of the local oscillator E_b is changed, one may measure an arbitrary quadrature of the field E_a. In actual experiments, the phase of the local oscillator is adjusted to yield the maximum possible quadrature squeezing. The shot-noise level is determined by blocking the signal field, so that only the local oscillator field reaches the detector. The results of the measurements are spectrally analyzed, leading to the determination of the amount of squeezing as a function of the frequency. In practice, one deals with a continuum of modes, and the above analysis applies to the situation when the frequency window of the detector is much smaller than the linewidth of the light which is being measured.

III. REPRESENTATIONS IN PHASE SPACE

A. The density operator

We present in this section a brief review of the concept of density operator. For a pure state $|\psi\rangle$, the density operator is defined by

$$\hat{\rho} = |\psi\rangle\langle\psi| \,.$$

If instead one is uncertain about the state of the system, and we know that there is a probability P_ψ for the system to be in state $|\psi\rangle$, the density operator is defined by

$$\hat{\rho} = \sum_\psi P_\psi |\psi\rangle\langle\psi| \,. \tag{35}$$

The utility of the above definitions can be grasped by writing down, in terms of $\hat{\rho}$, the average value of an observable $\hat{A}$:

$$\langle\hat{A}\rangle = \sum_\psi P_\psi \langle\psi|\hat{A}|\psi\rangle = \mathrm{Tr}(\hat{\rho}\hat{A}) \,, \tag{36}$$

which represents a unified way of expressing the average value, valid both for a pure state and a statistical mixture.

¿From the definition it follows immediately that $\mathrm{Tr}\hat{\rho} = \sum_\psi P_\psi = 1$.

Also, it is easy to see that $\hat{\rho}$ is Hermitian, and therefore can be diagonalized. If $|\phi_i\rangle$ are the eigenstates of $\hat{\rho}$, then

$$\hat{\rho} = \sum_i P_i |\phi_i\rangle\langle\phi_i| \,, \quad \langle\phi_i|\phi_j\rangle = \delta_{ij} \,,$$

which implies that

$$\hat{\rho}^2 = \sum_i P_i^2 |\phi_i\rangle\langle\phi_i| \Rightarrow \mathrm{Tr}\hat{\rho}^2 = \sum_i P_i^2 \leq 1 \,.$$

For a pure state, $\mathrm{Tr}\left(\hat{\rho}^2\right) = 1$, while for a mixture $\mathrm{Tr}\left(\hat{\rho}^2\right) < 1$.

In terms of the Fock basis,

$$\hat{\rho} = \sum_{nm} \rho_{nm} |n\rangle\langle m| \,.$$

Finally, let us recall that if one has two systems (interacting or not), let us say an atom and an electromagnetic field, a basis for the combined system can be obtained by forming the tensor product of the bases corresponding to each of the two systems. The tensor product of two states $|\psi_A\rangle$ and $|\psi_F\rangle$ corresponding respectively to the systems A and F is written as

$$|\psi_A\rangle \otimes |\psi_F\rangle \,,$$

corresponding to the density operator

$$\hat{\rho} = \hat{\rho}_A \otimes \hat{\rho}_F \,.$$

The average of expressions involving products of operators acting on A and on F separately can be written as

$$\langle\hat{A}\hat{F}\rangle = \mathrm{Tr}(\hat{\rho}_A\hat{A})\mathrm{Tr}(\hat{\rho}_F\hat{F}) \,.$$

Of course, a general state of the combined system will not have the form of a tensor product, but can be expressed as a linear combination of tensor product states. A state which cannot be factorized is called an *entangled state*.

States may also be represented by phase space distributions, which allow quantum-mechanical averages of operators to be expressed as classical-like integrations over phase space of c-numbers corresponding to the operators. In these lectures, we will pay special attention to the Wigner distribution.

B. The Wigner distribution

Phase space probability distributions are very useful in classical statistical physics. Averages of relevant functions of the positions and momenta of the particles can be obtained by integrating these functions with those probability weights.

In quantum mechanics, similar averages are calculated through Eq. (36). Heisenberg's inequality forbids the existence in phase space of bonafied probability distributions, since one cannot determine simultaneously the position and the momentum of a particle. In spite of this, phase space distributions may still play a useful role in quantum mechanics, allowing the calculation of the average of operator-valued functions of the position and momentum operators as classical-like integrals of c-number functions. These functions are associated to those operators through correspondence rules, which depend on a previously defined operator ordering.

¿From all phase space representations, the Wigner distribution is the most natural, when one looks for a quantum-mechanical analog of a classical probability distribution in phase space. This is a consequence of a beautiful result demonstrated by Bertrand and Bertrand [20], which will be presented here. The following account stays close to the ones in Refs. [16] and [20].

Let us look for a representation for which the *marginal distributions* coincide with the quadrature probability distributions:

$$\int dp\, W(q,p) = \langle q|\hat{\rho}|q\rangle\,, \int dq W(q,p) = \langle p|\hat{\rho}|p\rangle\,. \tag{37}$$

One should note that, for a pure state, $\langle q|\hat{\rho}|q\rangle = |\psi(q)|^2$, $\langle p|\hat{\rho}|p\rangle = |\tilde{\psi}(p)|^2$. One should also note that from (37) it follows immediately the normalization property:

$$\int dpdq\, W(q,p) = 1\,. \tag{38}$$

Properties (37) must remain true if one rotates the axes in phase space, so that

$$\hat{q}_\theta = \hat{U}^\dagger(\theta)\hat{q}\,\hat{U}(\theta) = \hat{q}\cos\theta + \hat{p}\sin\theta\,, \tag{39}$$

$$\hat{p}_\theta = \hat{U}^\dagger(\theta)\hat{p}\,\hat{U}(\theta) = -\hat{q}\sin\theta + \hat{p}\cos\theta\,, \tag{40}$$

or, inversely,

$$\hat{q} = \hat{q}_\theta\cos\theta - \hat{p}_\theta\sin\theta\,, \tag{41}$$

$$\hat{p} = \hat{q}_\theta\sin\theta + \hat{p}_\theta\cos\theta\,. \tag{42}$$

Thus:

$$P(q_\theta) = \int W(q_\theta\cos\theta - p_\theta\sin\theta, q_\theta\sin\theta + p_\theta\cos\theta)dp_\theta\,, \tag{43}$$

where now

$$P(q_\theta) = \langle q|\hat{U}(\theta)\hat{\rho}\,\hat{U}^\dagger(\theta)|q\rangle\,. \tag{44}$$

Expression (43), which yields the probability distribution for q_θ in terms of the function $W(q,p)$, is called a *Radon transform*. It was investigated in 1917 by the mathematician Johan Radon [21], who showed that, if one knows $P(q_\theta)$ for all angles θ, then one can uniquely recover $W(q,p)$, through the so-called *Radon inverse transform*. In one now identifies $P(q_\theta)$, given by the Radon transform (43), with the quantum expression (44), then it follows that (43) and (44) uniquely determine the function $W(q,p)$, in terms of the density operator $\hat{\rho}$ of the system. The function $W(q,p)$ is in this case precisely the Wigner function of the system.

Before demonstrating this result, let us note that Radon's result is the mathematical basis of tomography. In fact, application of this procedure to medicine (see Fig. 3) has brought the Nobel prize in Medicine to the medical doctors Cormack and Hounsfield in 1979.

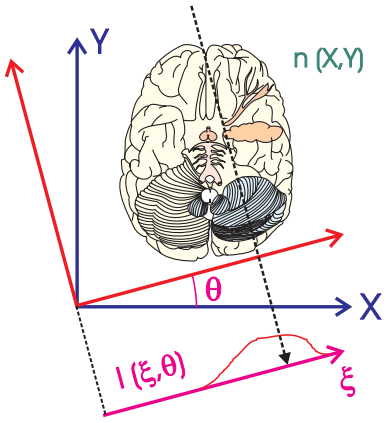

FIG. 3. Medical tomography. Measurement of the X-ray absorption for all angles along a plane allows one to reconstruct the absorptive part of the refraction index for a slice of the organ under investigation.

C. Reconstruction of the Wigner function

It is shown now that the distribution $W(q,p)$ may be uniquely determined from the knowledge of $P(q_\theta)$. For this end, let us introduce the *characteristic function* corresponding to $W(q,p)$, which is just the Fourier transform of this distribution:

$$\tilde{W}(u,v) = \int\int W(q,p)\exp(-iuq - ivp)\,dq\,dp\,. \tag{45}$$

The characteristic function corresponding to $P(q_\theta)$ is introduced in a similar way:

$$\tilde{p}(\xi,\theta) = \int P(q_\theta)\exp(-i\xi q_\theta)\,dq_\theta\,. \tag{46}$$

Inserting in (46) the expression for $P(q_\theta)$ as a function of W, given by (43), one gets:

$$\tilde{p}(\xi,\theta) = \int\int W(q,p)\exp(-i\xi q_\theta)dq_\theta\,dp_\theta\,,$$

where $q = q_\theta\cos\theta - p_\theta\sin\theta$ and $p = q_\theta\sin\theta + p_\theta\cos\theta$, and therefore $q_\theta = q\cos\theta + p\sin\theta$.

Changing the integration variables in $\tilde{p}(\xi,\theta)$, so that $(q_\theta, p_\theta) \to (q,p)$, one gets:

$$\tilde{p}(\xi,\theta) = \int_{-\infty}^{+\infty}\int_{-\infty}^{+\infty} W(q,p)\exp[-i\xi(q\cos\theta + p\sin\theta)]dq\,dp\,. \tag{47}$$

Therefore, $\tilde{p}(\xi,\theta)$ is the Fourier transform of $W(q,p)$ in polar coordinates:

$$\tilde{p}(\xi,\theta) = \tilde{W}(\xi\cos\theta, \xi\sin\theta)\,.$$

This implies that, from $P(q_\theta)$, one can calculate $\tilde{p}(\xi,\theta)$, and from this function one can calculate $W(q,p)$.

This demonstrates the tomographic reconstruction of $W(q,p)$. In order to connect this distribution to the density operator of the system, one uses Eq. (44):

$$\tilde{p}(\xi,\theta) = \int_{-\infty}^{+\infty}\langle q_\theta|\hat{\rho}|q_\theta\rangle e^{-i\xi q_\theta}\,dq_\theta = \int_{-\infty}^{+\infty}\langle q_\theta|\hat{\rho}e^{-i\xi\hat{q}_\theta}|q_\theta\rangle dq_\theta = \mathrm{Tr}\left[\hat{\rho}e^{-i\xi\hat{q}_\theta}\right]\,. \tag{48}$$

But $\xi\hat{q}_\theta = \hat{q}\xi\cos\theta + \hat{p}\xi\sin\theta$. Therefore, setting $u = \xi\cos\theta$, $v = \xi\sin\theta$, one gets

$$\tilde{W}(u,v) = \mathrm{Tr}\left[\hat{\rho}e^{-iu\hat{q}-iv\hat{p}}\right]\,.$$

Another form for the $W(q,p)$ can be obtained in the following way. We rewrite the characteristic function $\tilde{W}(u,v)$ as:

$$\tilde{W}(u,v) = \int_{-\infty}^{+\infty} \langle q|\hat{\rho}e^{-iu\hat{q}-iv\hat{p}}|q\rangle\, dq = e^{iuv/2}\int_{-\infty}^{+\infty} \langle q|\hat{\rho}e^{-iu\hat{q}}|q+v\rangle\, dq$$
$$= \int_{-\infty}^{+\infty} e^{-iux}\left\langle x - \frac{v}{2}\,|\hat{\rho}|\, x + \frac{v}{2}\right\rangle\, dx\,, \tag{49}$$

where we have used that

$$\exp(-iu\hat{q} - iv\hat{p}) = \exp(-iuv/2)\exp(-iu\hat{q})\exp(-iv\hat{p})$$

and we have set $q = x - v/2$. Taking the Fourier transform of $\tilde{W}(u,v)$ given by (49), one gets the following expression for the distribution $W(q,p)$:

$$W(q,p) = \frac{1}{2\pi}\int_{-\infty}^{+\infty} e^{ipx}\left\langle q - \frac{x}{2}\,|\hat{\rho}|\, q + \frac{x}{2}\right\rangle\, dx\,, \tag{50}$$

which, except for a normalization constant, is the famous expression written down by Wigner [22] in his article *"On the Quantum Correction for Thermodynamic Equilibrium"*, published in 1932. Wigner used this quasi-probability distribution in phase space as a convenient way of calculating quantum corrections to classical statistical mechanics. He wrote in his paper that (50) "was chosen from all possible expressions, because it seems to be the simplest." He added a quite intriguing footnote: "This expression was found by L. Szilard and the author some years ago for another purpose." One has shown here that the Wigner distribution has in fact a quite distinctive feature: it is the only distribution in phase space which yields the correct marginal distributions for any quadrature!

The tomographic procedure has a simple interpretation for a harmonic oscillator. From (10), it is clear that in this case measuring the quadratures for all angles is equivalent to measuring the position of the harmonic oscillator for all times from 0 to $2\pi/\omega$. This implies that the measurement of $|\psi(x,t)|^2$ for $0 < t \leq 2\pi/\omega$ allows one to reconstruct the state $\psi(x,t)$ of the harmonic oscillator.

The question about what is the minimum set of measurements needed to reconstruct the state of a system is actually a very old problem in quantum mechanics. In his article on quantum mechanics in the *Handbuch der Physik* in 1933 [15], Pauli stated that "the mathematical problem, as to whether for given functions $W(x)$ and $\tilde{W}(p)$ [probability distributions in position and momentum space], the wave function ψ, if such a function exists, is always uniquely determined has still not been investigated in all its generality." One knows now the answer to this question: the probability distributions $W(x)$ and $\tilde{W}(p)$ do not form a complete set in the tomographic sense, and therefore are not sufficient to determine uniquely the quantum state of the system.

D. Expression of the Wigner function in terms of $\hat{a}$ and $\hat{a}^\dagger$

Setting

$$\hat{q} = \frac{1}{\sqrt{2}}\left(\hat{a} + \hat{a}^\dagger\right), \quad \hat{p} = \frac{i}{\sqrt{2}}\left(\hat{a}^\dagger - \hat{a}\right), \quad \lambda = \frac{1}{\sqrt{2}}(u + iv)\,, \tag{51}$$

one gets

$$\tilde{W}(\lambda,\lambda^*) = \mathrm{Tr}\left(\hat{\rho}e^{-i\lambda^*\hat{a} - i\lambda\hat{a}^\dagger}\right). \tag{52}$$

The Fourier transform of this expression yields the Wigner function, expressed in terms of $\hat{a}$ and $\hat{a}^\dagger$:

$$W(\alpha,\alpha^*) = \frac{1}{\pi}\int d^2\lambda\, e^{\alpha\lambda^* - \alpha^*\lambda}\tilde{W}(\lambda,\lambda^*)\,. \tag{53}$$

This expession may be written in a very simple form, by using that

$$\int d^2\lambda\, e^{-a|\lambda|^2 + \mu\lambda + \nu\lambda^*} = \frac{\pi}{a}e^{\mu\nu/a}\,. \tag{54}$$

It follows that

$$W(\alpha,\alpha^*) = 2\left\langle : e^{-2(\hat{a}^\dagger - \alpha^*)(\hat{a} - \alpha)} : \right\rangle = 2\left\langle \hat{D}^\dagger(\alpha,\alpha^*) : e^{-2\hat{n}} : \hat{D}(\alpha,\alpha^*)\right\rangle, \tag{55}$$

where $\hat{D}(\alpha,\alpha^*) = \exp(\alpha\hat{a}^\dagger - \alpha^*\hat{a})$ is the displacement operator. We use now the identity:

$$t^{\hat{n}} =: e^{(t-1)\hat{n}} :, \tag{56}$$

which may be easily proven by applying both sides to an arbitrary Fock state. We get then [23]:

$$W(\alpha,\alpha^*) = 2\left\langle \hat{D}(\alpha,\alpha^*)(-1)^{\hat{n}}\hat{D}^{-1}(\alpha,\alpha^*)\right\rangle = 2\mathrm{Tr}\left[\hat{\rho}\hat{D}(\alpha,\alpha^*)e^{i\pi\hat{a}^\dagger\hat{a}}\hat{D}^{-1}(\alpha,\alpha^*)\right]. \tag{57}$$

Since $\exp(i\pi a^\dagger a)$ is the parity operator, this expression shows that the Wigner function is proportional to the average of the displaced parity operator.

The Wigner function given by (57) involves actually a different normalization with respect to the one defined before: one must set $W \to 2\pi W$, so that

$$\int (d^2\alpha/\pi)\, W(\alpha,\alpha^*) = 1\,. \tag{58}$$

E. Properties of the Wigner distribution

Thorough discussions of properties of the Wigner distribution can be found in Refs. [16] and [24]. Here only some of them are summarized.

It is easy to show that the Wigner function is real and bounded. If one adopts the normalization of (50), so that (38) holds, then Schwarz's inequality implies that $|W(q,p)| \leq 1/\pi$. If the Cahill-Glauber normalization (57) is adopted instead, so that (58) is satisfied, one has $|W(\alpha,\alpha^*)| \leq 2$.

Furthermore, let $W_\psi(q,p)$ be the Wigner function corresponding to the state $\psi(q)$, and $W_\phi(q,p)$ the Wigner function corresponding to the state $\phi(q)$, as given by (50). Then,

$$\left|\int dq\, \psi^*(q)\phi(q)\right|^2 = 2\pi \int dq \int dp\, W_\psi W_\phi\,.$$

This relation has several consequences. First, setting $\psi(q) = \phi(q)$, one gets $\int dq \int dp\, [W(q,p)]^2 = 1/2\pi$. More generally, it is easy to show that

$$\mathrm{Tr}\left(\hat{\rho}^2\right) = 2\pi \int\int dq\, dp\, [W(q,p)]^2\,, \tag{59}$$

and therefore $\int\int dq\, dp\, [W(q,p)]^2 < 1/2\pi$ for a statistical mixture. It is also clear that

$$\int dq \int dp\, W_\psi W_\phi = 0 \quad \text{if } \langle\psi|\phi\rangle = 0\,, \tag{60}$$

which implies that W cannot be always positive. This may be thought as a consequence of the Heisenberg inequalities: since it is not possible to measure simultaneously q and p, one cannot have in quantum mechanics bonafied probability distributions in phase space. In fact, one can show that the only pure states leading to positive-definite Wigner functions correspond to Gaussian wave functions [25]. This is the case for coherent states, and also for squeezed states.

One should note that the Husimi distribution, often found in the literature, and defined by $Q(\alpha,\alpha^*) = \langle\alpha|\hat{\rho}|\alpha\rangle/\pi$, is always positive, but does not lead to the correct marginal distributions.

F. Averages of operators

As shown by Moyal in 1949 [26], the Wigner distribution can be used to calculate averages of symmetric operator functions of q and p, as classical-like integrals in phase space. Thus, for instance,

$$\mathrm{Tr}\left(\hat{\rho}\left\{\hat{q}^2\hat{p}\right\}_{\mathrm{sim}}\right) = \mathrm{Tr}\left[\hat{\rho}\left(\hat{q}^2\hat{p} + \hat{q}\hat{p}\hat{q} + \hat{p}\hat{q}^2\right)/3\right] = \int dqdp\, W(qp)q^2p\,. \tag{61}$$

The association of a symmetrized quantum operator to a classical function is called *Weyl correspondence*.

This property of the Wigner function can be shown by considering the two equivalent expressions for the characteristic function $\tilde{W}(u,v)$,

$$\tilde{W}(u,v) = \mathrm{Tr}\left[\hat{\rho}e^{-iu\hat{q}-iv\hat{p}}\right] ,$$

$$\tilde{W}(u,v) = \int\int W(q,p)\exp(-iuq-ivp)\,dq\,dp\,,$$

from which one gets

$$\mathrm{Tr}\left[\hat{\rho}(\mu\hat{q}+\nu\hat{p})^k\right] = i^k\frac{\partial^k}{\partial\xi^k}\tilde{W}(\xi\mu,\xi\nu)\bigg|_{\xi=0} = \int_{-\infty}^{+\infty} W(q,p)(\mu q+\nu p)^k dq\,dp\,. \tag{62}$$

Comparing powers of μ and ν, one gets

$$\mathrm{Tr}\left(\hat{\rho}\left\{\hat{q}^m\hat{p}^n\right\}_{\mathrm{sim}}\right) = \int_{-\infty}^{+\infty} W(q,p)q^m p^n\,dq\,dp\,.$$

Of course, the same property holds for the Wigner function expressed in terms of $\hat{a}$ and $\hat{a}^\dagger$. Thus, for instance,

$$\mathrm{Tr}[\hat{\rho}(\hat{a}\hat{a}^\dagger+\hat{a}^\dagger\hat{a})/2] = \int(d^2\alpha/\pi)\,\alpha\alpha^* W(\alpha,\alpha^*)\,. \tag{63}$$

Other distributions in phase space can be introduced, which allow writing as classical-like integrals averages of functions of the operators $\hat{a}$ and $\hat{a}^\dagger$ written in normal and anti-normal order. Thus, for instance, the Husimi distribution can be shown to correspond to operators in anti-normal order. These distributions will not be discussed here [27].

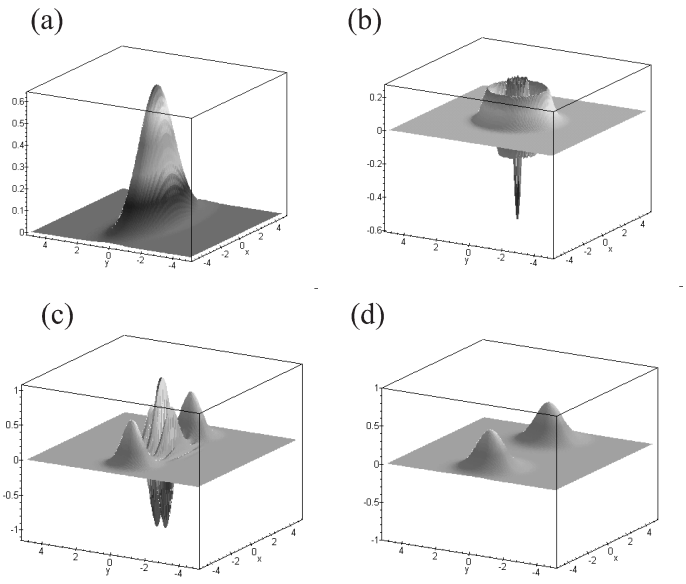

FIG. 4. Examples of Wigner distributions. (a) Squeezed state; (b) Fock state with $n = 3$; (c) Superposition of two coherent states, $|\psi\rangle \propto |\alpha_0\rangle + |-\alpha_0\rangle$, with $\alpha_0 = 3$; (d) Statistical mixture $(|\alpha_0\rangle\langle\alpha_0| + |-\alpha_0\rangle\langle-\alpha_0|)/2$, also with $\alpha_0 = 3$.

G. Examples of Wigner functions

Wigner functions corresponding to special states of the electromagnetic field can be obtained from either (50) or (57). We adopt in this section the normalization corresponding to (50).

For the vacuum state, one has the Gaussian

$$W_0(q,p) = \frac{1}{\pi} e^{-q^2-p^2} \,. \tag{64}$$

The Wigner function for a coherent state can be easily obtained by applying a displacement to the above Gaussian:

$$W_c(q,p) = \frac{1}{\pi} e^{-(q-q_0)^2-(p-p_0)^2} \,. \tag{65}$$

Application of a scaling transformation to (64) yields the Wigner function for a squeezed vacuum, plotted in Fig. 4(a):

$$W_\xi(q,p) = \frac{1}{\pi} \exp\left(-e^{2\xi} q^2 - e^{-2\xi} p^2\right) \,. \tag{66}$$

For a one-photon Fock state $|1\rangle$, one gets:

$$W_1(q,p) = \frac{1}{\pi} e^{-q^2-p^2} (2q^2 + 2p^2 - 1) \,. \tag{67}$$

This function vanishes for $\sqrt{q^2+p^2} = 1/\sqrt{2}$, and is negative at the origin of phase space. This negative value reminds us of the highly non-classical nature of a Fock state. For higher photon numbers, the Wigner function displays more oscillations, the number of zeros coinciding with n. Fig. 4(b) displays the Wigner function corresponding to a Fock state with $n = 3$.

Of special interest for our discussion on the classical limit of quantum mechanics is the state formed by superimposing two coherent states $|\alpha_0\rangle$ and $|-\alpha_0\rangle$ (setting $\alpha_0 = q_0$ real for simplicity):

$$|\psi\rangle = \mathcal{N}[|\alpha_0\rangle + |-\alpha_0\rangle] \,, \tag{68}$$

where $\mathcal{N}$ is a normalization constant, given by

$$\mathcal{N} = \left[2\left(1 + \exp(-2|\alpha_0|^2\right)\right]^{-1/2} \,. \tag{69}$$

The corresponding wave function in configuration space is given by

$$\psi(q) = \mathcal{N}\left[e^{-(q-q_0)^2/2} + e^{-(q+q_0)^2/2}\right] \,,$$

while the Wigner function is

$$W(q,p) = (\mathcal{N}/\pi)\left[e^{-(q-q_0)^2-p^2} + e^{-(q+q_0)^2-p^2} + 2e^{-q^2-p^2}\cos(2pq_0)\right] \,. \tag{70}$$

This function is displayed in Fig. 4(c).

It is interesting to compare this Wigner function with the one corresponding to a statistical mixture of the same coherent states, with equal weights:

$$\hat{\rho} = \tfrac{1}{2}\left(|\alpha_0\rangle\langle\alpha_0| + |-\alpha_0\rangle\langle-\alpha_0|\right) \,, \tag{71}$$

for which

$$W(q,p) = (1/2\pi)\left[e^{-(q-q_0)^2-p^2} + e^{-(q+q_0)^2-p^2}\right] \,. \tag{72}$$

This function is displayed in Fig. 4(d).

While (72) is just the sum of two Gaussians, corresponding to the coherent states $|\alpha_0\rangle$ and $|-\alpha_0\rangle$ respectively, (70) displays interference fringes around the origin of phase space, which is a clear signature of the coherence between the two states $|\alpha_0\rangle$ and $|-\alpha_0\rangle$ in (68). Therefore, the measurement of the Wigner function of the electromagnetic field would be a clear-cut way of distinguishing between a coherent superposition and a mixture of the two coherent states. It will be seen shortly that these two coherent states may be interpreted, within the framework of recent experiments in cavity QED, as pointers of a measuring apparatus. The mechanism by which a state like (68) loses its coherence, approaching state (71), is thus very relevant for the quantum theory of measurement.

H. Measurement of the Wigner function

The inverse Radon transform suggests that the Wigner function of an electromagnetic field can be reconstructed by determining $P(q_\theta)$ through homodyne detection [28]. This has actually been achieved in 1993 by Smithey *et al.* [29]. In view of the low detection efficiency in those experiments, the detected distribution was actually a smoothed version of the Wigner function, closely related to the Husimi distribution. A much better result was achieved by Mlynek's group in 1995 [30], clearly displaying a highly compressed Gaussian, corresponding to the experimentally obtained Wigner function of a squeezed state of light emerging from an optical parametric oscillator. A procedure closely related to the homodyne detection method was used to reconstruct the vibrational state of a molecule by T. J. Dunn *et al.* [31]

The Wigner function can also be obtained by measuring the populations of displaced states. Indeed, from (57), one has:

$$W(\alpha,\alpha^*) = \mathrm{Tr}\left[\hat{\rho}\hat{D}(\alpha,\alpha^*)e^{i\pi\hat{a}^\dagger\hat{a}}\hat{D}^{-1}(\alpha,\alpha^*)\right] = \sum_n \langle n|\hat{D}^{-1}(\alpha,\alpha^*)\hat{\rho}\hat{D}(\alpha,\alpha^*)e^{i\pi\hat{a}^\dagger\hat{a}}|n\rangle$$
$$= \sum_n (-1)^n \langle n|\hat{D}^{-1}(\alpha,\alpha^*)\hat{\rho}\hat{D}(\alpha,\alpha^*)|n\rangle\,. \tag{73}$$

If $\hat{\rho}$ corresponds to a mode of the electromagnetic field in a cavity, then $\hat{D}^{-1}(\alpha,\alpha^*)\hat{\rho}\hat{D}(\alpha,\alpha^*)$ can be obtained from $\hat{\rho}$ by injecting a coherent state into the cavity, through for instance the coupling of the cavity with a microwave generator (if the frequency of the mode in the cavity is in the microwave range). One must measure then the population of the displaced states, which can be done for instance by applying the procedure described in Ref. [33].

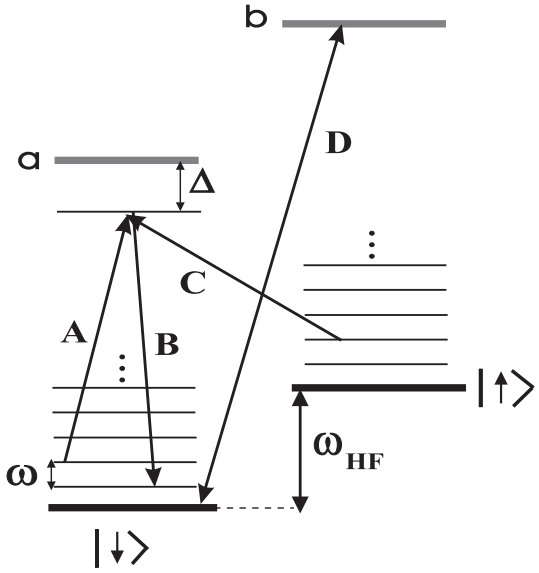

FIG. 5. Measurement of the Wigner function for a trapped ion, by Leibfried *et al.* Displacement of the vibrational state associated with the internal state $|\downarrow\rangle$ (a hyperfine structure sublevel) is achieved by applying fields A and B, which induce transitions between neighboring vibrational states corresponding to the electronic level $|\downarrow\rangle$, without changing the ion's internal state. Population of displaced states is measured by inducing a resonant exchange during a time t between states $|\downarrow, n\rangle$ and $|\uparrow, n+1\rangle$ with fields B and C (turning off field A). Probability of finding the atom in $|\downarrow\rangle$ as a function of t, determined by exciting it to level d (with a high fluorescence yield), leads to information on population of displaced vibrational states.

This method was used by Wineland's group at NIST to measure the Wigner function of vibrational states of a trapped ion [32]. The relevant level scheme is shown in Fig. 5. States $|\downarrow\rangle$ and $|\uparrow\rangle$ correspond to two metastable ground-state hyperfine sublevels ($^2S_{1/2}$, with $F=2$, $m_F=-2$ and $F=1$, $m_F=-1$, respectively), separated by $\hbar\omega_{HF}$. The ion is trapped in a harmonic potential, and the vibrational levels associated with each electronic state $|\downarrow\rangle$ and $|\uparrow\rangle$ are also sketched in Fig. 5. Initially, the ion is in the internal state $|\downarrow\rangle$. The displacement of the vibrational state in phase space is obtained by inducing a Raman transition between neighboring vibrational states, when the internal state of the ion is $|\downarrow\rangle$. This is accomplished by applying the two fields A and B illustrated in Fig. 5, with a frequency difference equal to the vibrational frequency ω. Beam B is circularly polarized (σ_-), and does not couple

$|\uparrow\rangle$ to any virtual $^2P_{1/2}$ state, so that only the motional state correlated with $|\downarrow\rangle$ is displaced. These fields do not lead to transitions between electronic levels of the trapped ion, since they are detuned with respect to the possible electronic transitions, and therefore they affect only the center-of-mass motion. The action of the two fields can thus be modeled by an effective Hamiltonian of the form $H \propto (\hat{a}+\hat{a}^\dagger)$, where $\hat{a}$ and $\hat{a}^\dagger$ are harmonic oscillator lowering and raising operators. The evolution operator corresponding to this Hamiltonian is precisely the displacement operator, therefore the Raman process induces a displacement of the original state in phase space. A resonant exchange between states $|\downarrow\rangle|n\rangle$ and $|\uparrow\rangle|n+1\rangle$ is then induced for a time t, with fields B and C (turning off field A). For each time t and each displacement α the population $P_\downarrow(t,\alpha)$ of the $|\downarrow\rangle$ state is measured. A fourth level b is used for detecting the electronic state of the ion (and also for Doppler precooling): a pulse D resonant with the $|\downarrow\rangle \leftrightarrow |b\rangle$ transition leads to a fluorescence signal if the ion is in $|\downarrow\rangle$, while the absence of fluorescence implies that the ion is in $|\uparrow\rangle$ (the detection efficiency for this process is close to 100%). The internal state at $t=0$ being always equal to $|\downarrow\rangle$, the signal averaged over many measurements is $P_\downarrow(t,\alpha) = \frac{1}{2}\left[1+\sum_{n=0}^{\infty} Q_n(\alpha)\cos(2\Omega_{n,n+1}t)e^{-\gamma_n t}\right]$, where $\Omega_{n,n+1}$ are the oscillation frequencies, γ_n their experimentally determined decay constants, and $Q_n(\alpha) = \langle n|\hat{D}^\dagger(\alpha)\hat{\rho}\hat{D}(\alpha)|n\rangle$ is the population distribution of the displaced state. The dependence of $\Omega_{n,n+1}$ on n allows the determination of $Q_n(\alpha)$ from $P_\downarrow(t,\alpha)$ [32], and from $Q_n(\alpha)$ one determines the Wigner function through Eq. (73).

It is clear that both methods are highly indirect. It will be shown in the following however that it is possible to conceive a much more direct method for measuring the Wigner function at any point in phase space, for either an electromagnetic field in a cavity or a trapped ion.

IV. THE ATOM-FIELD INTERACTION

A. The interaction Hamiltonian

We consider now the interaction of atoms and fields. We will be considering situations in which the atom is resonant or quasi-resonant with one of the modes of the electromagnetic field in a cavity. Under these conditions, it is possible to consider just two of the atomic states, and therefore reduce the atom to a two-level system (we will call e the upper level, and g the lower level). The basic Hamiltonian describing this system is

$$H = H_A + H_F + H_{AF}\,, \tag{74}$$

where

$$H_A = (\hbar\omega_0/2)\sigma_3 \tag{75}$$

is the free-atom Hamiltonian, with σ_3 a Pauli matrix:

$$\sigma_3 = \begin{pmatrix} 1 & 0 \\ 0 & -1 \end{pmatrix}\,, \tag{76}$$

$$H_F = \hbar\omega\left(a^\dagger a + \tfrac{1}{2}\right) \tag{77}$$

is the free-field Hamiltonian, and

$$H_{AF} = \hbar g(\sigma_+ a + \sigma_- a^\dagger)\,, \tag{78}$$

with

$$\sigma_+ = (\sigma_-)^\dagger = \begin{pmatrix} 0 & 1 \\ 0 & 0 \end{pmatrix}\,. \tag{79}$$

The real coupling constant $\hbar g$ depends on the transition dipole $\vec{d}_{ab}$ between the two levels, on the polarization vector $\vec{\epsilon}$ and the frequency ω of the electromagnetic field, as well as the effective volume of the mode V. From (6), it follows that

$$\hbar g = -\vec{d}_{ab}\cdot\vec{\epsilon}\sqrt{\frac{h\omega}{V}}u(\vec{R})\,, \tag{80}$$

where the mode function $u(\vec{R})$ is evaluated on the center-of-mass position ($\vec{R}$) of the atom interacting with the field. One should note that, since only two atomic states are involved, one may always choose their phases so that g is real. If $u(\vec{R})$ is real, then this choice will not depend on $\vec{R}$.

In Eq. (78), we neglected terms of the form $\sigma_+ a^\dagger$ and $\sigma_- a$, which do not conserve energy in first order, and which lead to small corrections in the results to be obtained, as long as $|\omega - \omega_0| \ll \omega_0$.

The above equations define the *Jaynes-Cummings model* [34], a very useful model in Quantum Optics, and which has described with success many experiments in cavity QED. One should note that this model neglects dissipative processes, which will be considered in a while.

B. Heisenberg equations of motion for atom and semiclassical approximation

¿From the above Hamiltonian, one gets the following equations of motion for the atomic operators:

$$\dot{\hat{\sigma}}_+ = i\omega_0 \hat{\sigma}_+ - ig\hat{a}^\dagger \hat{\sigma}_3 \,, \tag{81}$$

$$\dot{\hat{\sigma}}_3 = -2ig\left(\hat{\sigma}_+ \hat{a} - \hat{\sigma}_- \hat{a}^\dagger\right) . \tag{82}$$

The *semiclassical approximation* is obtained by setting $\hat{a} \to \alpha$, $\hat{a}^\dagger \to \alpha^*$, where α and α^* are c-numbers.

Adopting this approximation, one gets for the average values of the atomic operators, after applying the transformation $\alpha \to \alpha \exp(-i\omega t)$, $\hat{\sigma}_+ \to \hat{\sigma}_+ \exp(i\omega t)$:

$$\begin{aligned} \langle \dot{\hat{\sigma}}_+ \rangle &= i\delta \langle \hat{\sigma}_+ \rangle - ig\alpha^* \langle \hat{\sigma}_3 \rangle \,, \\ \langle \dot{\hat{\sigma}}_3 \rangle &= -2ig\left(\langle \hat{\sigma}_+ \rangle \alpha - \langle \hat{\sigma}_- \rangle \alpha^*\right) , \end{aligned} \tag{83}$$

where $\delta = \omega_0 - \omega$ is the detuning between the atom and the field.

C. Bloch equations

If one rewrites Eqs. (83) in terms of $r_1 \equiv \langle \hat{\sigma}_1 \rangle$, $r_2 \equiv \langle \hat{\sigma}_2 \rangle$, and $r_3 \equiv \langle \hat{\sigma}_3 \rangle$, with $g\alpha \equiv V/2 \equiv (V_1 - iV_2)/2$, one gets the *Bloch equations*, which can be written as:

$$\frac{d\vec{r}}{dt} = \vec{\Omega} \times \vec{r}, \tag{84}$$

where $\vec{r} = (r_1, r_2, r_3)$ and $\vec{\Omega} = (V_1, V_2, \delta)$.

In terms of the atomic density matrix,

$$\hat{\rho}_A = \begin{pmatrix} \rho_{ee} & \rho_{eg} \\ \rho_{ge} & \rho_{gg} \end{pmatrix} ,$$

one may write:

$$r_1 = \mathrm{Tr}(\hat{\sigma}_1 \hat{\rho}_A) = \rho_{eg} + \rho_{ge} = 2\Re e(\rho_{ge}) \tag{85}$$

$$r_2 = \mathrm{Tr}(\hat{\sigma}_2 \hat{\rho}_A) = i(\rho_{eg} - \rho_{ge}) = 2\Im m(\rho_{ge}) \tag{86}$$

$$r_3 = \mathrm{Tr}(\hat{\sigma}_3 \hat{\rho}_A) = \rho_{ee} - \rho_{gg} \tag{87}$$

These equations represent the atomic state by a pseudo-spin $\vec{r}$ (Bloch vector), which precesses around the pseudo-magnetic field $\vec{\Omega}$, as shown in Fig. 6. The precession frequency, given by

$$\Omega = \sqrt{|V|^2 + \delta^2} \,, \tag{88}$$

is the *Rabi frequency*. The vertical component of the Bloch vector represents the atomic population, while the equatorial projection is associated with the atomic polarization ($\vec{P}$ in Fig. 6). This picture of the evolution of a two-level atom is due to Feynman, Vernon, and Hellwarth [35].

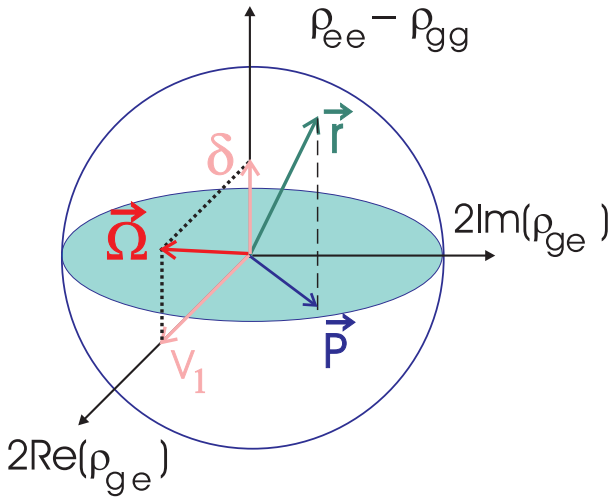

FIG. 6. Precession of the Bloch vector $\vec{r}$ around the pseudo-magnetic field $\vec{\Omega}$, with V real.

For a pure state, $|\psi\rangle = c_e|e\rangle + c_g|g\rangle$, one has

$$\hat{\rho}_A = \begin{pmatrix} |c_e|^2 & c_e^* c_g \\ c_e c_g^* & |c_g|^2 \end{pmatrix}, \quad r_1^2 + r_2^2 + r_3^2 = 1\,.$$

Therefore, in this case the tip of the Bloch vector is situated on a sphere of unit radius.

Two limiting cases of this expression correspond to the resonant and to the dispersive interaction. When the interaction is resonant, $\delta = 0$, $\vec{\Omega} = (V_1, V_2, 0)$. and the Bloch vector precesses around a vector in the equatorial plane. One gets in this case maximum population transfer. The precession frequency is then $|V|$. In the dispersive limit, $|\delta| \gg |V|$, and $\vec{\Omega} \to (0, 0, \delta)$. The Bloch vector precesses then around a vector parallel to the axis 3 (population axis), with a frequency equal to δ, as shown in Fig. 7.

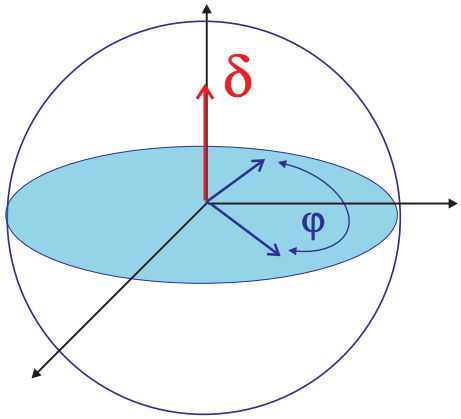

FIG. 7. Dispersive limit: the Bloch vector precesses around the vertical axis.

D. Quantum theory: the dressed atom

We go back now to the Hamiltonian (74), and consider the effects resulting from the quantization of the electromagnetic field.

The Hamiltonian (74) defines the *dressed atom* [36]. While H_A has two energy levels, H_F has an infinite number of discrete levels, given by $\hbar\omega(n + 1/2)$, $n = 0, 1, 2, \ldots$. The interaction H_{AF} couples these levels, leading to a discrete structure of levels of the composed system, which one could call the "atom-field molecule". We will study first the structure of the uncoupled system, and then we will analyze the energy levels of the coupled system.

1. Uncoupled states

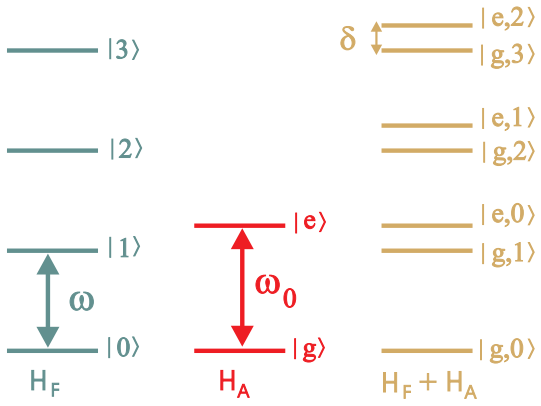

FIG. 8. Energy level diagram for the uncoupled atom-field system

The state in which the atom is in state e and the field has n photons will be denoted by $|e,n\rangle$. Analogously for $|g,n\rangle$. Let again $\delta = \omega_0 - \omega$ be the detuning between the atom and the field. If $|\delta| \ll \omega_0$, the states $|e,n\rangle$ and $|g,n+1\rangle$ will be very close to each other. If $\delta > 0$, the energy of the state $|g,n+1\rangle$ will be smaller than the energy of the state $|e,n\rangle$ (see Fig. 8). In fact, we can write

$$E_{e,n} = \hbar\omega(n+1) + \frac{\hbar\delta}{2}\,, \tag{89}$$

$$E_{g,n+1} = \hbar\omega(n+1) - \frac{\hbar\delta}{2}\,. \tag{90}$$

We have therefore a sequence of subspaces $\mathcal{E}(n) \equiv \{|g,n+1\rangle; |e,n\rangle\}$. Note that $E_{e,0} = \hbar(\omega+\omega_0)/2$, and $E_{g,0} = -\hbar\delta/2 = \hbar(\omega-\omega_0)/2$, consistently with the fact that the zero-point energy is $\hbar\omega/2$ and the energies of the two atomic states are $\pm\hbar\omega_0/2$.

2. Coupled states

The Hamiltonian (74), with H_{AF} given by (78), couples only states within the same subspace (this is a consequence of the rotating-wave approximation; the counter-rotating terms, neglected in H_{AF}, connect states belonging to different subspaces, which leads to small corrections to the results considered here, due to the large energy differences involved). Therefore, in order to calculate the eigenvalues of the complete Hamiltonian, one has to diagonalize a 2×2 matrix, given in the subspace $\mathcal{E}(n)$ by:

$$[H]_n = \hbar \begin{pmatrix} \omega(n+1) - \frac{\delta}{2} & g\sqrt{n+1} \\ g\sqrt{n+1} & \omega(n+1) + \frac{\delta}{2} \end{pmatrix}\,. \tag{91}$$

The eigenvalues of this matrix define the energy levels of the dressed atom:

$$E_{\pm,n} = (n+1)\hbar\omega \pm (\hbar\Omega/2)\,, \tag{92}$$

$$E_{g,0} = -\hbar\delta/2\,, \tag{93}$$

where

$$\Omega = \left[\Omega_0^2(n+1) + \delta^2\right]^{1/2} \tag{94}$$

is the quantum *Rabi frequency* of the system, while $\Omega_0 = 2g$ is the *vacuum Rabi frequency*, which coincides with Ω when $n = 0$ and $\delta = 0$. The quantum Rabi frequency (94) coincides precisely with the classical expression (88) if one identifies $\Omega_0\sqrt{n+1}$ with $|V|$. One should note however that, contrary to the classical expression, the quantum Rabi

frequency remains different from zero even when the number of photons in the mode is equal to zero. The remaining contribution is associated with spontaneous emission into the mode, which couples the state $|e,0\rangle$ to the state $|g,1\rangle$.

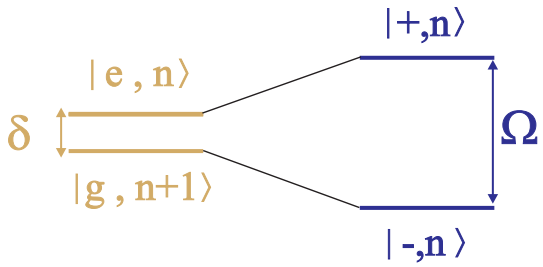

FIG. 9. Energy displacement of levels, produced by the coupling.

The expression (92) shows that the two states are separated by the coupling, the energy difference between them going from $\hbar\delta$ to $\hbar\Omega$. This effect is displayed in Fig. 9.

The corresponding eigenstates are given by:

$$|+,n\rangle = \sin\theta|g,n+1\rangle + \cos\theta|e,n\rangle\,, \tag{95}$$
$$|-,n\rangle = \cos\theta|g,n+1\rangle - \sin\theta|e,n\rangle\,, \tag{96}$$

with

$$\cot 2\theta = \frac{\delta}{\Omega_0\sqrt{n+1}}\,, \quad 0 \le 2\theta < \pi\,. \tag{97}$$

3. Resonant interaction

At resonance, $\delta = 0$, and therefore $\theta = \pi/4$, so that

$$|+,n\rangle = \frac{1}{\sqrt{2}}\left(|g,n+1\rangle + |e,n\rangle\right)\,, \tag{98}$$
$$|-,n\rangle = \frac{1}{\sqrt{2}}\left(|g,n+1\rangle - |e,n\rangle\right)\,. \tag{99}$$

In this case, each subspace $\mathcal{E}(n)$ becomes two-fold degenerate, and the dressed states are expressed in terms of the sum and the difference of the corresponding uncoupled states, with equal weights. The corresponding energies are, for $n \neq 0$,

$$E_{\pm,n} = (n+1)\hbar\omega \pm (\hbar\Omega_0\sqrt{n+1}/2)\,. \tag{100}$$

4. Dispersive interaction

For large detuning ($|\delta| \gg \Omega_0\sqrt{n+1}$), one gets $\theta \to \pi/2$ if $\delta < 0$, and $\theta \to 0$ if $\delta > 0$, and therefore

$$|+,n\rangle \to |g,n+1\rangle\,, \quad |-,n\rangle \to |e,n\rangle\,, \quad (\delta < 0)\,, \tag{101}$$
$$|+-n\rangle \to |e,n\rangle\,, \quad |-,n\rangle \to |g,n+1\rangle\,, \quad (\delta > 0)\,. \tag{102}$$

These equations show that, for a dispersive interaction, the coupled states approach the uncoupled states, with an energy shift obtained from (92):

$$E_{\pm,n} \approx (n+1)\hbar\omega \pm (\hbar\omega/2)|\delta| \pm \hbar\Omega_0^2(n+1)/4|\delta|\,. \tag{103}$$

In any case, we have in this limit:

$$\Delta E_{e,n} \approx \hbar(\Omega_0^2/4\delta)(n+1)\,, \tag{104}$$
$$\Delta E_{g,n} \approx -\hbar(\Omega_0^2/4\delta)n\,. \tag{105}$$

The two energy levels of each subspace get displaced in opposite directions. This displacements coincide precisely with those which would be obtained using second-order perturbation theory, and constitute the *Stark effect*.

E. Dynamics of the interaction

Once the Hamiltonian is diagonalized, one can easily describe the dynamical behavior of the system. From (95), one has:

$$|e,n\rangle = \cos\theta|+,n\rangle - \sin\theta|-,n\rangle\,, \tag{106}$$
$$|g,n+1\rangle = \sin\theta|+,n\rangle + \cos\theta|-,n\rangle\,, \tag{107}$$

and therefore, if the initial state of the system is $|\psi(0)\rangle = |e,n\rangle$, we will have at time t:

$$|\psi(t)\rangle = \cos\theta e^{-iE_{+,n}t/\hbar}|+,n\rangle - \sin\theta e^{-iE_{-,n}t/\hbar}|-,n\rangle\,, \tag{108}$$

or yet, reexpressing in terms of the uncoupled states:

$$\begin{aligned}|\psi(t)\rangle = e^{-i\omega(n+1)t}\big\{ &-i\sin(2\theta)\sin(\Omega t/2)|g,n+1\rangle \\ &+ [\cos(\Omega t/2) - i\cos(2\theta)\sin(\Omega t/2)]\,|e,n\rangle\big\}\,.\end{aligned} \tag{109}$$

The probabilities of finding the system in the states $|e,n\rangle$ e $|g,n+1\rangle$ are given by

$$P_{e,n} = \cos^2(\Omega t/2) + \cos^2(2\theta)\sin^2(\Omega t/2)\,, \tag{110}$$
$$P_{g,n+1} = \sin^2(2\theta)\sin^2(\Omega t/2)\,, \tag{111}$$

oscillating therefore with the Rabi frequency Ω. At resonance, when $\theta = \pi/4$, one gets, except for the overall phase factor $\exp[-i\omega(n+1)t]$:

$$|\psi(t)\rangle = -i\sin(\Omega t/2)|g,n+1\rangle + \cos(\Omega t/2)|e,n\rangle\,, \tag{112}$$

and therefore $P_{e,n} = \cos^2(\Omega t/2)$, $P_{g,n+1} = \sin^2(\Omega t/2)$, so the oscillation has maximum amplitude. For $\Omega t = \pi/2$, one gets a superposition with equal probabilites of the states $|e,n\rangle$ and $|g,n+1\rangle$. Furthermore, for a full turn of the Bloch vector ($\Omega t = 2\pi$), one gets from (112): $|\psi(t)\rangle \to -|e\rangle|n\rangle$. Therefore, $|\psi(t)\rangle$ comes back to the initial state, but with a minus sign, which is typical of spin-1/2 systems.

These considerations extend to the quantum case the description of the atomic evolution in terms of the Bloch vector, previously discussed within the semiclassical approximation. One should note that, if one starts from the state $|e,n\rangle$, the quantum system evolves even when the number of photons in the mode is equal to zero, contrary to what would happen if the field is not quantized. This extra quantum feature is again due to spontaneous emission by the atomic excited state into the cavity mode.

One should also note that, in the dispersive limit, neither the number of photons nor the populations of states e and g change, exactly as in the semiclassical treatment. In this case, the dynamics of the atom is well represented by the precession of the Bloch vector around the vertical axis (population axis): if there are n photons in the field, the angle of precession is given by $(\Delta E_{e,n} - \Delta E_{g,n})t/\hbar$, with the Stark energy displacements given by (104).

V. COHERENT SUPERPOSITIONS OF MESOSCOPIC STATES IN CAVITY QED

A. Building the coherent superposition

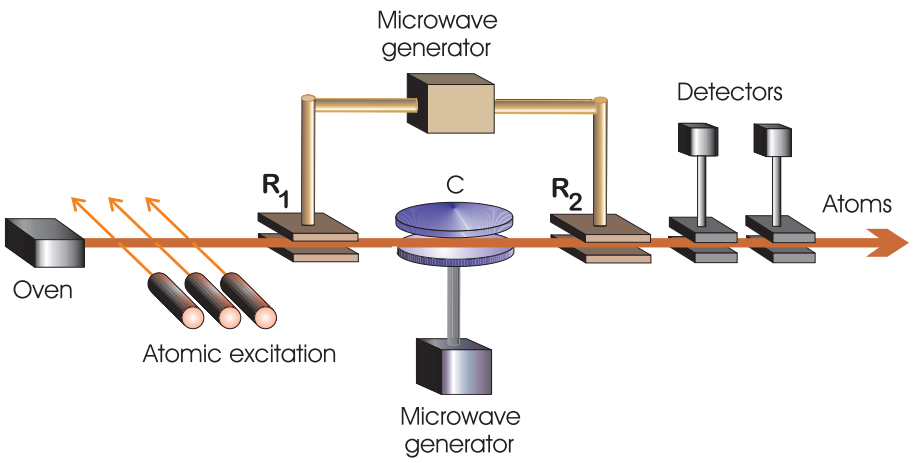

FIG. 10. Experimental arrangement for producing and measuring a coherent superposition of two coherent states of the field in cavity **C**.

We show now how, by carefully tailoring the interactions between two-level atoms and one mode of the electromagnetic field in a cavity, one can produce quantum superpositions of distinguishable coherent states of the field, thus mimicking the superposition of two classically distinct states of a pointer.

The method, proposed in Ref. [33], and sketched in Fig. 10, involves a beam of circular Rydberg atoms [37] crossing a high-Q cavity in which a coherent state is previously injected (this is accomplished by coupling the cavity to a classical source – a microwave generator – through a wave guide). The utilization of circular levels is due to their strong coupling to microwaves and their very long radiative decay times, which makes them ideally suited for preparing and detecting long-lived correlations between atom and field states [38]. On either side of the high-Q cavity there are two low-Q cavities ($\mathbf{R_1}$ and $\mathbf{R_2}$), which remain coupled to a microwave generator. The fields in these two cavities can be considered as classical. This set of two low-Q cavities constitutes the usual experimental arrangement in the Ramsey method of interferometry [38,39]. Two of the atomic levels, which we denote by $|e\rangle$ and $|g\rangle$, are resonant with the microwave fields in cavities $\mathbf{R_1}$ and $\mathbf{R_2}$, the intensity of these fields being such that, for the selected atomic velocity, effectively a $\pi/2$ pulse is applied to the atom as it crosses those cavities. For a properly chosen phase of the microwave field, this pulse transforms the state $|e\rangle$ into the linear combination $(|e\rangle + |g\rangle)/\sqrt{2}$, and the state $|g\rangle$ into $(-|e\rangle + |g\rangle)/\sqrt{2}$.

Therefore, if each atom is prepared in the state $|e\rangle$ just prior to crossing the system, after leaving $\mathbf{R_1}$ the atom is in a superposition of two circular Rydberg states $|e\rangle$ and $|g\rangle$:

$$|\psi_{\rm atom}\rangle = \frac{1}{\sqrt{2}}(|e\rangle + |g\rangle)\,. \tag{113}$$

On the other hand, the superconducting cavity is assumed not to be in resonance with any of the transitions originating from those two atomic states. This means that the atom does not suffer a transition, and does not emit or absorb photons from the field. This property is further enhanced by the fact that the cavity mode is such that the field slowly rises and decreases along the atomic trajectory, so that, for sufficiently slow atoms, the atom-field coupling is adiabatic. However, the cavity is tuned in such a way that it is much closer to resonance with respect to one of those transitions, say the one connecting $|e\rangle$ to some intermediate state $|i\rangle$. The relevant level scheme is illustrated in Fig. 11. This implies that, if the atom crosses the cavity in state $|e\rangle$, dispersive effects can induce an appreciable phase shift on the field in the cavity. The phase shift is negligible, however, if the atom is in state $|g\rangle$. For a principal quantum number equal to 50 in the state e, and the cavity tuned close to the $50 \rightarrow 51$ circular to circular transition (around 50 GHz), a phase shift of the order of π is produced by an atom crossing the centimeter size cavity with a velocity of about 100 m/s [33].

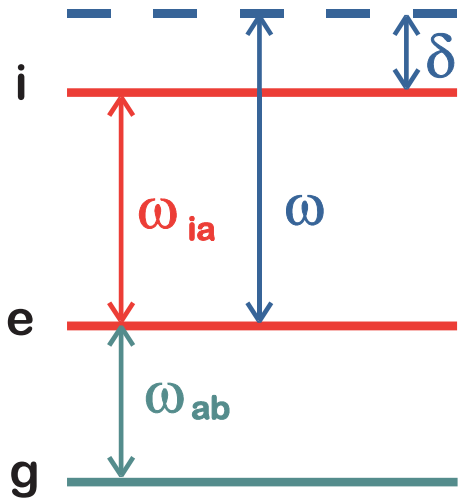

FIG. 11. Atomic level scheme. The transition $i \leftrightarrow e$ is detuned by δ from the frequency ω of a mode of cavity **C**, while the transition $e \leftrightarrow g$ is resonant with the fields in $\mathbf{R_1}$ and $\mathbf{R_2}$. State $|g\rangle$ is not affected by the field in **C**.

After the atom has crossed the cavity, in a time short compared to the field relaxation time and also to the atomic radiative damping time, the state of the combined atom-field system can be written as

$$|\psi_{\text{atom+field}}\rangle = \frac{1}{\sqrt{2}}(|e;-\alpha\rangle + |g;\alpha\rangle)\,, \tag{114}$$

assuming that the phase shift is π if the atom is in the excited state. The entanglement between the field and atomic states is analogous to the correlated two-particle states in the Einstein-Podolski-Rosen (EPR) paradox [40–42]. The two possible atomic states e and g are here correlated to the two field states $|-\alpha\rangle$ and $|\alpha\rangle$, respectively, which may be considered as macroscopic pointers (if $|\alpha| \gg 1$). After the atoms leave the superconducting cavity, one can detect them in the e or g states, by sending them through two ionization chambers, the first one having a field smaller than the second, so that it ionizes the atom in the e state, but not in the g state, while the second ionizes the atoms which remain in state g (Fig. 10). This measurement projects the field in the cavity either in the $|\alpha\rangle$ (if the atom is detected in state g), or in the $|-\alpha\rangle$ state (if the atom is detected in state e). However, as in an EPR experiment [42], one may choose to make another kind of measurement, letting the atom cross, after it leaves the superconducting cavity, a second classical microwave field ($\mathbf{R_2}$ in Fig. 10), which amounts to applying to the atom another $\pi/2$ pulse. The state (114) gets transformed then into

$$|\psi'_{\text{atom+field}}\rangle = \tfrac{1}{2}\left(|e;-\alpha\rangle - |e;\alpha\rangle + |g;\alpha\rangle + |g;-\alpha\rangle\right)\,. \tag{115}$$

If one detects now the atom in the state $|g\rangle$ or $|e\rangle$, the field is projected onto the state

$$|\psi_{\text{cat}}\rangle = \frac{1}{N_1}\left(|\alpha\rangle + e^{i\psi_1}|-\alpha\rangle\right)\,, \tag{116}$$

where $N_1 = \sqrt{2\left[1+\cos\psi_1 \exp(-2|\alpha|^2|)\right]}$ and $\psi_1 = 0$ or π, according to whether the detected state is g or e, respectively. One produces therefore a coherent superposition of two coherent states, with phases differing by π. For $|\alpha|^2 \gg 1$, this is a "Schrödinger cat" state.

Superpositions of coherent states of the field were produced in the experiment reported in Ref. [43], and were detected by a procedure which can be considered, as shown in the next Section, as a special case of a method for measuring the Wigner function of the field in the cavity.

B. Effect of dissipation

Before considering how these states can be detected, we discuss the effect of dissipation, due to imperfections in the mirrors and diffraction losses. A simple model for dissipation is obtained by coupling the field oscillator (of frequency ω) to a bath of harmonic oscillators, which represent the modes of the reservoir. We consider here for simplicity a rotating-wave Hamiltonian, and a zero-temperature bath. The method here exposed, and which results from joint

work of the author with V. M. Kenkre, can be easily generalized to account for a finite-temperature bath [44]. The corresponding Hamiltonian may be written as

$$H = \hbar\omega a^{\dagger}a + \sum_{q} \hbar\omega_{q} b_{q}^{\dagger} b_{q} + \hbar \sum_{q} \left(G_{q} a^{\dagger} b_{q} + G_{q}^{*} a b_{q}^{\dagger} \right) , \tag{117}$$

where G_q are the coupling constants, and the bath oscillators have frequency ω_q.

It is straightforward to write down the evolution equation for the Heisenberg operators $a(t)$, $b_q(t)$, and their adjoints. Since the resulting equations are linear, they may be solved by the Laplace transform method.

The explicit solution for $a(t)$ is given by

$$a(t) = a(0)\,\xi(t) + \sum_{q} \eta_{q}(t)\, b_{q}(0) . \tag{118}$$

The Laplace transforms of the c-number functions $\xi(t)$ and $\eta_q(t)$ appearing in (118) are given respectively by

$$\tilde{\xi}(s) = \left[s + i\omega + \tilde{\phi}(s) \right]^{-1} , \tag{119}$$

$$\tilde{\eta}_{q}(s) = -iG_{q} \left(s + i\omega_{q} \right)^{-1} \left[s + i\omega + \tilde{\phi}(s) \right]^{-1} . \tag{120}$$

The function ϕ which appears in both (119) and (120) reflects the nature of the coupling and is given in the time domain by

$$\phi(t) = \sum_{q} |G_{q}|^{2} e^{-i\omega_{q} t} = \int_{0}^{\infty} d\nu\, \mathcal{G}(\nu)\, e^{-i\nu t} . \tag{121}$$

In the second equality in (121) we have introduced the quantity $\mathcal{G}(\nu)$ which equals the product of the coupling $|G_q|^2$ assumed to be a function of the frequency alone, and the density of states $\sum_q \delta(\nu - \omega_q)$ of the b-oscillators.

Since the total number of oscillator excitations in both oscillators, $a^{\dagger}a + \sum_q b_q^{\dagger} b_q$, commutes with the Hamiltonian and is therefore an invariant, it follows that

$$|\xi(t)|^{2} + \sum_{q} |\eta_{q}(t)|^{2} = 1 . \tag{122}$$

In order to get now the time-dependent Wigner function, it suffices to replace the solution (118) in the characteristic function (52), and then calculate the Wigner function through (53). Assuming that the initial state of the field in the cavity is given by (68), one gets then:

$$W(\alpha, \alpha^{*}, t) = \frac{2}{\mathcal{N}^{2}} \left\{ e^{-2|\alpha - \xi(t)\alpha_{o}|^{2}} + e^{-2|\alpha + \xi(t)\alpha_{o}|^{2}} + 2F(t) \right\} , \tag{123}$$

where the normalization factor $\mathcal{N}$ is given by (69). Here, the fringe function $F(t)$ is given by

$$F(t) = \exp\left\{ -2 \left[|\alpha_{0}|^{2} \left(1 - |\xi(t)|^{2} \right) + |\alpha|^{2} \right] \right\} \cos\left\{ 4\alpha_{0} \mathrm{Im}\left[\alpha \xi^{*}(t) \right] \right\} . \tag{124}$$

The Markoffian limit corresponds to setting $\phi(t) = \Gamma\delta(t)$, which implies that

$$\xi(t) = e^{-i\Omega t} e^{-\Gamma t} . \tag{125}$$

More generally, one could have a frequency shift as well, in the Markoffian limit, arising from the fact that the integration in (121) is from zero to infinity. It is clear then from (124) and (125) that, for $\Gamma t \ll 1$, the fringe function decays very fast, in a time scale of the order of $1/2|\alpha_0|^2\Gamma$. This shows explicitly that the term associated with coherence decays at a much faster rate than the energy of the system, if $|\alpha_0|^2 \gg 1$. As the distance between the two coherent states increases, this effect becomes more and more pronounced, and the coherent superposition of the two "pointers" becomes practically indistinguishable from a statistical mixture: this is the reason why such coherent superpositions are extremely difficult to observe in the macroscopic world! The physical origin of the decoherence process is actually very simple: as the field in the cavity leaks into the external reservoir, the states of the field get correlated with states of the reservoir which become approximately orthogonal after the time it takes for one photon

to leave the cavity, thus implying the disappearance of interference effects between the two internal states. This can be clearly seen, if one assumes that the decoherence time depends only on the distance between the two states in phase space, upon displacing the initial state in the cavity by α_0, so that the state $|\psi'\rangle = (1/\mathcal{N})[|2\alpha_0\rangle + |0\rangle]$ is obtained (which has the same distance between the two states of the superposition as the original state). For the state $|2\alpha_0\rangle$, a photon leaves the cavity in a time of the order of $(1/4|\alpha_0|^2\Gamma)$, while for the state $|0\rangle$ no photon leaves the cavity. Since the probability for finding the system in each of these states is $1/2$ for $|\alpha_0| \gg 1$, it follows that the effective lifetime of a photon is $(1/2|\alpha_0|^2\Gamma)$, which is precisely the decoherence time: after this time, the state $|2\alpha_0\rangle$ becomes correlated with a state of the reservoir containing approximately one photon, while the state $|0\rangle$ remains correlated with the vacuum. Decoherence of the system under observation is therefore closely connected with entanglement between this system and the reservoir.

VI. DIRECT MEASUREMENT OF THE WIGNER FUNCTION

Once the proper state of the field is produced in the cavity, how would one be able to measure it? As shown in [45], it is actually possible to measure the Wigner function of the field by a relatively simple scheme, which provides directly the value of the Wigner function at any point of phase space. This is in contrast with the tomographic procedure, or the method based on the measurement of populations adopted at NIST, which yield the Wigner function only after some integration or summation. Furthermore, and also in contrast with those methods, the present scheme is not sensitive to detection efficiency, as long as one atom is detected within a time shorter than the decoherence time. A similar procedure can be applied to the reconstruction of the vibrational state of a trapped ion [45], and also in some cases to molecules [46]. We will discuss here only the application to the electromagnetic field.

The basic experimental scheme for measuring the Wigner function [45] coincides with the one used to produce the "Schrödinger cat"-like state, illustrated in Fig. 10. A high-Q superconducting cavity $\mathbf{C}$ is placed between two low-Q cavities ($\mathbf{R_1}$ and $\mathbf{R_2}$ in Fig. 10). The cavities $\mathbf{R_1}$ and $\mathbf{R_2}$ are connected to the same microwave generator, the field in $\mathbf{R_2}$ being dephased by η with respect to the field in $\mathbf{R_1}$. Another microwave source is connected to $\mathbf{C}$, allowing the injection of a coherent state in this cavity, so that the density operator $\hat{\rho}$ of the field to be measured is transformed into $\hat{\rho}' = \hat{D}(z, z^*)\hat{\rho}\hat{D}^{-1}(z, z^*)$. This system is crossed by a velocity-selected atomic beam, such that an atomic transition $e \leftrightarrow g$ is resonant with the fields in $\mathbf{R_1}$ and $\mathbf{R_2}$, while another transition $e \leftrightarrow i$ is quasi-resonant (detuning δ) with the field in $\mathbf{C}$, so that the atom interacts dispersively with this field if it is in state e, while no interaction takes place in $\mathbf{C}$ if the atom is in state g. The relevant level scheme is shown in Fig. 11. Just before $\mathbf{R_1}$, the atoms are promoted to the highly excited circular Rydberg state $|e\rangle$ (typical principal quantum numbers of the order of 50, corresponding to lifetimes of the order of some milliseconds). As each atom crosses the low-Q cavities, it sees a $\pi/2$ pulse, so that $|e\rangle \rightarrow [|e\rangle + \exp(i\eta)|g\rangle]/\sqrt{2}$, and $|g\rangle \rightarrow [-\exp(-i\eta)|e\rangle + |g\rangle]/\sqrt{2}$, with $\eta = 0$ in $\mathbf{R_1}$. If the atom is in state e when crossing $\mathbf{C}$, there is an energy shift of the atom-field system (Stark shift), which dephases the field, after an effective interaction time $t_{\rm int}$ between the atom and the cavity mode. The one-photon phase shift is given by $\phi = (\Omega^2/\delta)t_{\rm int}$, where the Rabi frequency Ω measures the coupling between the atom and the cavity mode. The atom is detected and the experiment is repeated many times, for each amplitude and phase of the injected field z, starting from the same initial state of the field $\hat{\rho}$. In this way, the probabilities P_e and P_g of detecting the probe atom in states e or g are determined. It is easy to show that

$$P_g - P_e = \Re e \left\{ e^{i\eta} \mathrm{Tr} \left[\hat{D}(z, z^*)\hat{\rho}\hat{D}^{-1}(z, z^*) e^{i\phi a^\dagger a} \right] \right\} . \tag{126}$$

Setting $\eta = 0$ and $\phi = \pi$, we can see from (57) that

$$P_g - P_e = W(-z, -z^*)/2. \tag{127}$$

Therefore, the difference between the two probabilities yields a direct measurement of the Wigner function (one should note that, due to the fact that here $|g\rangle$ does not interact with the field in $\mathbf{C}$, this expression differs from the one given in Ref. [45]).

An important feature of this scheme is the insensitivity to the detection efficiency of the atomic counters (of the order of 40±15% in recent experiments [33]). Indeed, if an atom is not detected after interacting with the cavity mode, the next atom will find a field described by the reduced density operator obtained from the entangled atom-field density matrix by tracing out the atomic states: $\hat{\rho}' \rightarrow \hat{\rho}'' = \frac{1}{2}(\hat{\rho}' + \hat{\mathcal{T}}_e\hat{\rho}'\hat{\mathcal{T}}_e^\dagger)$, where $\hat{\mathcal{T}}_e(\phi) = \exp(i\phi\hat{a}^\dagger\hat{a})$ is the phase shift operator associated with level e. The value of $P_g - P_e$ for this second atom is then easily shown to reduce to (127).

The measurement accuracy does depend however on the detector's selectivity, that is, the ability to distinguish between the two atomic states. Another possible source of error is the velocity spread of the atomic beam, which

would produce an uncertainty in the angle ϕ and in the angles of rotation in $\mathbf{R_1}$ and $\mathbf{R_2}$. For a 1% velocity spread and for average photon numbers of the order of 10, one can show that the distortion is at most equal to 0.04, in the relevant region of phase space, so that the measured distribution is practically undistinguishable from the true one. In fact, the insensitivity of the proposed scheme to the detection efficiency allows a passive selection of atomic velocity (only the atom which goes through the detectors at the right time after excitation is detected), which can be made with high precision.

One should note that this method allows the measurement of the Wigner function at each time t, allowing therefore the monitoring of the decoherence process "in real time". It is interesting, in this respect, to compare the procedure described above with the one suggested by Davidovich *et al* [47], with the objective of observing the decoherence of a Schrödinger cat-like state. In that reference, it was proposed that the decoherence of the state $|\pm\rangle = (|\alpha\rangle \pm |-\alpha\rangle)/N_{\pm}$ could be observed by measuring the joint probability of detecting in states $|e\rangle$ or $|g\rangle$ a pair of atoms, both prepared in the state $|e\rangle$ initially, and sent through the system depicted in Fig. 10. The atomic configuration considered in that reference coincides with the one adopted here. Detection of the first atom prepares the coherent superposition of coherent states, as described above. Detection of the second atom probes the state produced in **C**. Since no field was injected into the cavity between the two atoms, it is clear now that the experiment proposed in Ref. [47] amounts to a measurement of the Wigner function at the origin, which is non zero for the pure state $|\pm\rangle$, as shown in Fig. 4 (c), vanishes after the decoherence time (shorter than the intensity decay time by the factor $|\alpha|^2$), as shown in Fig. 4 (d), and increases again as dissipation takes place, bringing the field to the vacuum state. Following this proposal, the first observation of decoherence was realized by Brune *et al* [33]. In the experiment, both $|e\rangle$ and $|g\rangle$ lead to dephasings (in opposite directions) of the field in **C**. In this case, it is easy to show that the Wigner function is again recovered, as long as the one-photon phase shift is $\phi = \pi/2$ (with opposite signs for e and g), and a dephasing $\eta = \pi/2$ is applied to the second Ramsey zone [45]. This condition was not satisfied however in the experiment reported in Ref. [33]: due to experimental limitations, the angle ϕ was actually smaller than $\pi/2$. One expects however that this condition will be attained very soon.

VII. WIGNER FUNCTION AND CONTROLLED-NOT GATES

We show now that a simple experiment leads to the measurement of negative values for the Wigner function associated with a quantum state of the electromagnetic field in a cavity. The experiment is realized in two steps. In the first step, the two Ramsey zones are inactive, and a resonant atom in state $|e\rangle$ is sent through the high-Q cavity **C** (vacuum state inside), its interaction time being such that the atom suffers a transition to state $|g\rangle$ and one photon is left in the cavity. Such an experiment has been done recently by Maître *et al* [48]. One should note that it is relatively easy to tune the atom in and out of resonance with the cavity mode, by Stark shifting the atomic transition with the help of electric fields applied across the gap between the mirrors. [48] Having thus constructed the one-photon Fock state, one proceeds as described above, sending a second atom which crosses the two Ramsey zones and the high-Q cavity, where it interacts dispersively with the field, producing a dephasing equal to π per photon if the atom is in level e, and leaving the field unchanged if it is in level g (our scheme is easily adapted to the case in which both atomic levels lead to a phase shift of the field in the cavity). We do not apply any displacement field, so that, according to (127), the quantity $P_e - P_g$ yields the Wigner function at the origin of phase space. Since the Wigner function of a one-photon state is given by $W(z, z^*) = 2e^{-|z|^2}(2|z|^2 - 1)$, it is clear that $W(0) = -2 < 0$. This implies, according to (127), that $\Delta P = 1$, that is, the non-classical character of the state, associated to the negative value of the corresponding Wigner function at the origin of phase space, is translated, in this proposed experiment, into the fact that the probe atom comes out from the second Ramsey zone always in the upper state!

This result has a simple geometrical interpretation, in terms of the Bloch vector associated with the two-level atom, as shown in Fig. 12: the final position of the Bloch vector depends on whether the number of photons in the cavity is odd or even, and this at the origin of the manifestation of the non-classical behavior of the field. It follows immediately that the Wigner functions corrresponding to the states $|-\rangle$ and $|+\rangle$ have negative and positive values at the origin, respectively. One should note that the dependence on the photon number parity of the final atomic state leads to a controlled-not logic gate (a basic ingredient in quantum computation): the atomic state does not change if there is one photon in the cavity, while the absence of photons in the cavity leads to a change of atomic state. We have therefore the situation in which the state of one of the bits (0 or 1 photon in the cavity) controls what happens to the other bit (atom in the $|e\rangle$ or in the $|g\rangle$ state). This quantum-optics realization of a controlled-not gate was proposed in Ref. [11] as a basic ingredient for the teleportation of atomic states. We see that, in the present context, it is associated to the measurement of a striking non-classical manifestation of a Fock state: the negative value of the corresponding Wigner function at the origin of phase space. In the classical limit, attained for coherent states with an average number of photons much larger than one, odd and even photon populations come up with approximately the

same weight, implying that there is an equal probability that the atom comes up in the e or in the g state. Therefore, $\Delta P = 0$, corresponding to the well-known fact that the Wigner function of a coherent state with average number of photons much larger than one is practically equal to zero at the origin of phase space.

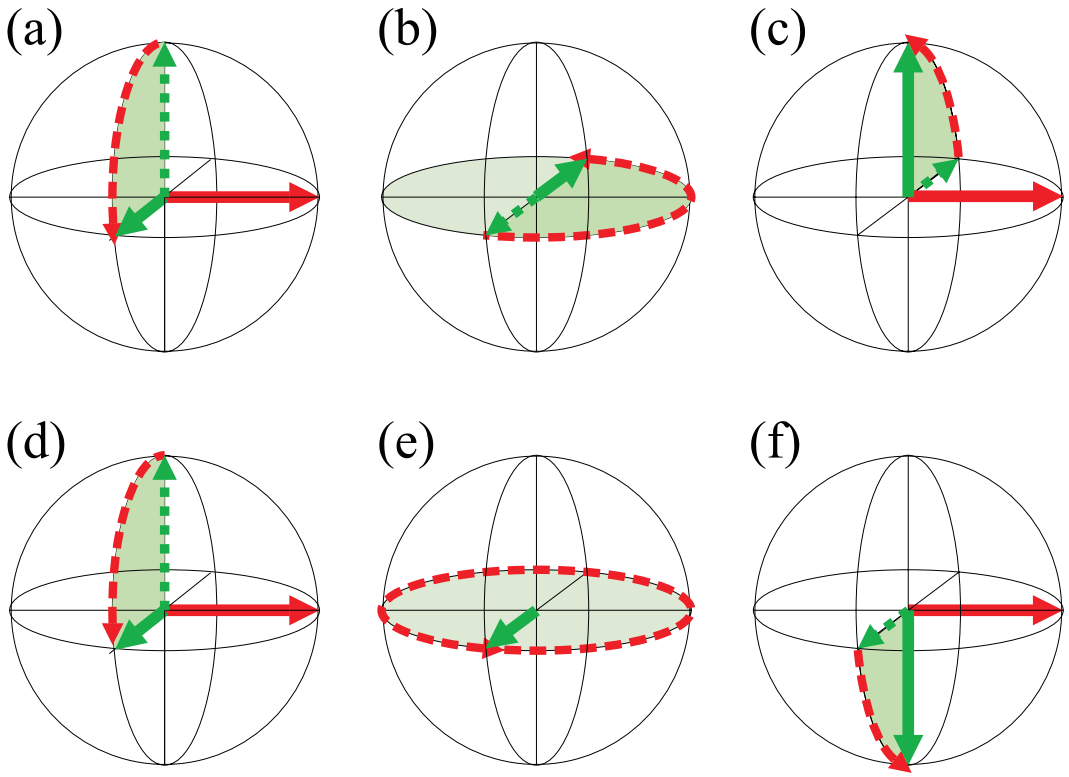

FIG. 12. Evolution of the Bloch vector (V) of an atom that crosses the proposed setup, interacting with the eletromagnetic field (E) in the two Ramsey zones, and having a dispersive interaction with the field in the superconducting cavity **C**, when the number of photons of the field in **C** has a well defined parity. The atom is initially in the state e. As the atom crosses the first Ramsey zone, its Bloch vector is rotated by $\pi/2$ around the vector representing the electromagnetic field along the real polarization axis, as shown in (a) and (d). As the atom crosses the cavity **C**, the Bloch vector rotates around the population axis. If the number of photons in the cavity is odd (b), the Bloch vector ends up pointing towards the opposite direction, and the rotation in the second zone leads the atom back to state $|e\rangle$ (c). On the other hand, if the number of photons in C is even, the Bloch vector turns by an integer multiple of 2π, so its direction does not change (d). The second Ramsey zone then brings the atom to $|g\rangle$ (f).

VIII. MEASUREMENT OF A NEGATIVE VALUE FOR THE WIGNER FUNCTION OF RADIATION

Recently, and using the above ideas, one was able to measure the Wigner function at the origin of phase space for a single photon field [49]. Its negative value exhibited the non-classical nature of this state. The experiment, realized at the Ecole Normale Supérieure in Paris, relied on an absorption-free detection of the microwave field stored in a superconducting cavity.

The heart of the method was the absorption-free detection of a single photon stored in a microwave cavity, reported recently in Nature [50]. One first used a "source" atom to prepare a one-photon field [48]. A "meter" atom then measured the field parity and hence the Wigner function at the origin. A "probe" atom finally checked the cavity state at the end of the experiment. This third atom allowed one to reject most errors due to cavity relaxation. This was an essential feature in this experiment.

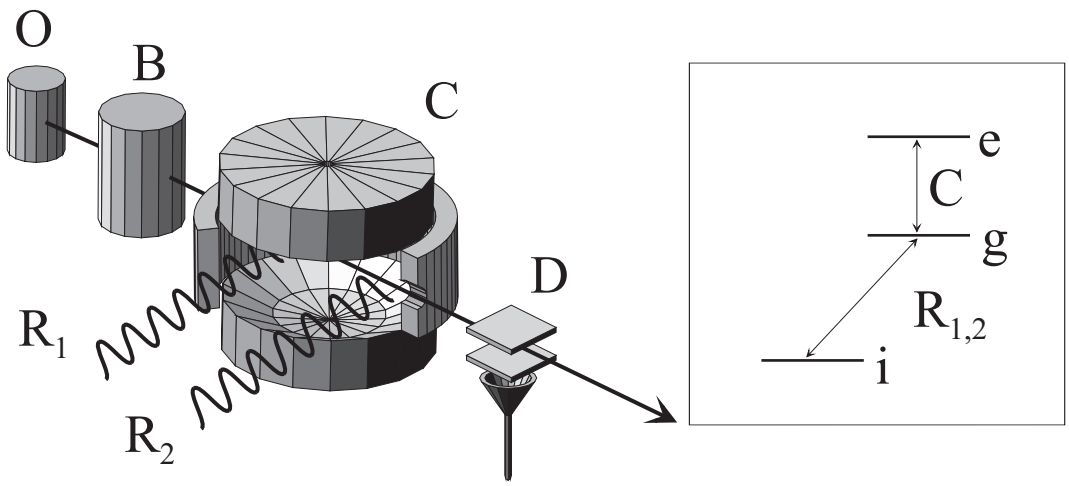

FIG. 13. Experimental setup for measuring the Wigner function of a one-photon Fock state at the origin of phase space.

Let us review first the principle of the single-photon detection [50]. Figure 13 presents the scheme of the experiment, with the relevant atomic states in the inset. One should note that the experimental arangement differs from the one discussed before, in that the Ramsey regions are now inside the superconducting cavity, which is encircled by a cylindrical wall, so as to minimize diffraction losses. This wall has small holes which allow the atoms to enter the cavity. Due to stray fields, however, coherence is destroyed when the atoms cross the holes, so it is necessary to make all coherent manipulations while the atom is in the cavity. The meter atom is prepared in the intermediate level g. A first $\pi/2$ microwave pulse R_1, resonant with the $g \Rightarrow i$ transition, prepares the superposition $(|g\rangle + |i\rangle)/\sqrt{2}$. The meter then interacts with the cavity C, resonant on the $g \Rightarrow e$ transition. When C contains no photon, or when the meter is in state i, the meter state is unaffected. When C contains one photon, the meter in level g undergoes a quantum Rabi nutation between g and e. The atom-cavity interaction time is adjusted for a 2π rotation. The $|g,1\rangle$ state is thus transformed into $-|g,1\rangle$. The photon is left in C and the atomic superposition becomes $(-|g\rangle + |i\rangle)/\sqrt{2}$. The meter states $|g\rangle$ and $|i\rangle$ are then mixed again by another $\pi/2$ pulse R_2, which realizes, together with R_1, a Ramsey interferometer [39]. The phase of R_2 is set so that it performs the transformations $(|g\rangle - |i\rangle)/\sqrt{2} \rightarrow |g\rangle$ and $(|g\rangle + |i\rangle)/\sqrt{2} \rightarrow |i\rangle$. The final meter state is thus i (g) when the photon number is 0 (1).

Provided the cavity state is in the $\{|0\rangle, |1\rangle\}$ subspace, the difference $P_i - P_g$ of the probabilities for detecting the atom in i or g is equal to the mean value of $\hat{P}$, i.e. half the Wigner function at origin:

$$W(0) = 2(P_i - P_g) = 2 - 4P_g\,. \tag{128}$$

Let us stress that this method only applies in the $\{|0\rangle, |1\rangle\}$ subspace. For larger fields, the 2π Rabi pulse condition is not enforced for all photon numbers and the atomic state is not simply related to $\hat{P}$. Thus, W cannot be measured at points different from the origin, since the required field displacement would take it outside this subspace.

In the experiment made at Ecole Normale, the levels e, g and i are the Rubidium circular levels with principal quantum numbers 51, 50 and 49 respectively. Three velocity-selected atomic samples, corresponding to the source, meter and probe, are prepared in box B in an atomic beam effusing from oven O. Each of them contains much less than one atom on the average, so that two-atom events for a single sample are negligible. The cavity C is made of two spherical niobium mirrors in a Fabry Perot configuration. It sustains a Gaussian mode (waist $w = 6$ mm) resonant with the $e \Rightarrow g$ transition (51.1 GHz). The single-photon Rabi frequency at cavity center is $\Omega/2\pi = 47$ kHz [38]. The atomic velocity is $V = 503(\pm 2.5)$ ms^{-1}, corresponding to an effective interaction time $t_i = \sqrt{\pi}w/V$ such that $\Omega t_i = 2\pi$. The mirrors are surrounded by a cylindrical ring with 3-mm holes for atom access. This ring reduces photon losses and increases the photon decay time up to 1 ms. A small electric field is applied across the mirrors. It is used to Stark-tune the atomic frequency in or out of resonance with C. The atom-cavity interaction time can thus be reduced to any fraction of t_i. The 54.3 GHz Ramsey pulses R_1 and R_2, resonant with the $g \Rightarrow i$ transition, are applied to the atoms inside the cavity structure. The final states of the atoms are analyzed in the field-ionization detector D.

The experiment was performed with the $|0\rangle$ and $|1\rangle$ states. One first gets rid of a 0.7 photon thermal field by a cooling procedure described in [50]. The residual photon number is less than 0.1. The initial field state is then produced by the source atom, which is prepared in e. It enters C 75 μs after the end of the cooling sequence and undergoes a $\pi/2$ spontaneous emission pulse in it. Either it is detected in e (50% of the cases), leaving C empty, or in

g, preparing a single photon. In this way, the Wigner functions for the $|0\rangle$ and $|1\rangle$ states are recorded simultaneously. The meter and probe are sent 100 μs and 175 μs after the source. The probe is prepared in g. It undergoes a π Rabi rotation in $|1\rangle$. Hence, ideally, the probe is detected in g if C is empty and in e if C contains one photon. When the detected states of the source and probe agree (either (eg) or (ge)), the probability of a photon number change induced by cavity relaxation is considerably reduced. Thus, the detection of the probe performs a "post-selection" of the field state experienced by the meter. This is a major improvement with respect to our previous experiments [50]. One should stress that this post-selection is only made possible by the non-demolition measurement of the field parity by the meter.

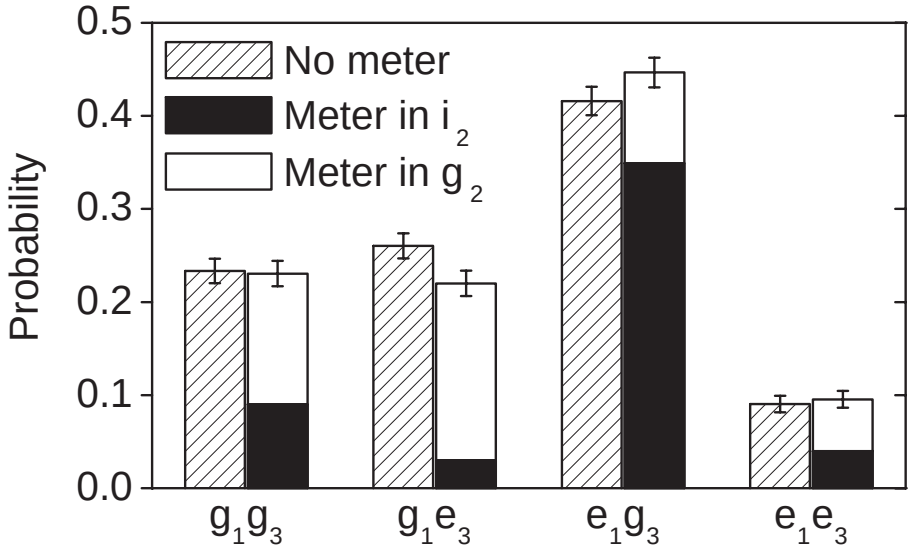

FIG. 14. Histograms giving the detection probabilities (about 1000 coincidences detected). Hatched bars: detection probabilities for the four possible output channels for the source and probe atom when no meter atom is sent through C. Black and white bars: detection probabilities for the source and probe conditioned to the state of the meter atom (i_2 and g_2 respectively). The error bars are statistical.

Figure 14 presents the observed atomic correlations. The hatched histograms give the probabilities for the detection of the source and probe in the four possible channels *when no meter atom is sent*. One thousand two-atoms coincidences have been recorded in about twenty minutes. Ideally, channels g_1e_3 and e_1g_3 should have identical 0.5 probabilities. The populations of the other channels (g_1g_3 and e_1e_3) mainly originate from cavity relaxation. Photon decay populates g_1g_3 from g_1e_3 (the probability of a decay between the source and the probe is 16%). Appearance of a thermal photon accounts in part for the population of the channel e_1e_3 (the corresponding probability is 13%). Other imperfections contribute also (thermal photon already present in C before the source, two-atoms events in one sample, detectors imperfections...).

The results obtained when the meter is sent trough C are displayed by the black and white histograms. About 1000 three-atoms coincidences have been recorded in 2 hours. These histograms give the probabilities to get one of the eight possible outcomes. The two bars corresponding to a given configuration of the source and probe are stacked. Each white bar corresponds to a meter detected in g_2, while the black ones correspond to a meter in i_2.

We observe that, within statistical errors (depicted by the error bars in fig. 3), the stacked black and white boxes have the same height as the corresponding hatched one. Hence, the meter does not alter the detection probabilities for the source and the probe and thus leaves the photon number unchanged [50]. For the g_1e_3 case (1 photon in C), the meter is detected mainly in g_2, in agreement with the settings of the Ramsey pulses (see above). Alternatively, it is detected most often in i_2 in the e_1g_3 case (empty cavity). The spurious channels mainly correspond to the absorption (g_1g_3) or to the creation (e_1e_3) of a photon. This occurs with equal probabilities before or after the meter has crossed C. In these cases, the meter is detected with almost equal probabilities in g_2 or i_2.

The relevant conditional probabilities are easily computed. The probability for detecting the meter in g_2 provided

the cavity contains one photon (g_1e_3 case) is $P(g_2|g_1e_3) = 0.83(4)$. In a similar way, the probability for detecting the meter in g_2 in the empty cavity case (e_1g_3 case) is found to be $P(g_2|e_1g_3) = 0.22(3)$. These figures are consistent with the 20% error rate of the single-photon absorption-free detection reported in [50]. From equation (128), we infer the values of $W(0)$ in the zero and one photon cases:

$$W_0(0) = 1.12(12) \tag{129}$$

$$W_1(0) = -1.32(16)\ . \tag{130}$$

Even though the ± 2 theoretical values are not reached due to the finite (60%) contrast of the Ramsey interferometer, the negativity of the Wigner function of a single photon field at the origin of phase space is clearly demonstrated.

The efficiency of the error rejection provided by the third atom can be estimated. If we discard the probe information, we get for the relevant conditional probabilities $P(g_2|g_1) = 0.71(4)$ for the one-photon case and $P(g_2|e_1) = 0.27(3)$ for the vacuum case, leading to the values $W_0(0) = 0.88(16)$ and $W_1(0) = -0.87(12)$. The quality of the Wigner function determination is thus considerably improved by the probe atom detection.

This experiment also provides a scheme for preparing a three-atom entangled state. Ideally, the source atom should be entangled with the cavity field after the $\pi/2$ Rabi rotation [48,51]. Since the whole evolution is then a coherent process, it leads to the preparation a Greenberger-Horne-Zeilinger entangled state [57]: $(|e_1, i_2, g_3\rangle - |g_1, g_2, e_3\rangle)/\sqrt{2}$. The entanglement of the three atoms was revealed in a recent experiment [53].

IX. WIGNER FUNCTION AND ENTANGLEMENT

The Wigner function may also be useful to characterize entanglement between two or more particles, or modes of the electromagnetic field. In fact, it was shown by K. Banaszek and K. Wódkiewicz [54] that Bell-type inequalities can be established between four points of the two-mode Wigner function corresponding to the maximally entangled state $(|1\rangle|0\rangle - |0\rangle|1\rangle)/\sqrt{2}$, which involves Fock states of the electromagnetic field.

More generally, it is possible to show that the Wigner function may provide a quantitative measurement of the entanglement between two Fock states of the electromagnetic field [55].

The two-mode Wigner function can be written as

$$W(\alpha, \beta) = tr\{\rho\widehat{\Pi}(\alpha, \beta)\} \tag{131}$$

where $\widehat{\Pi}(\alpha, \beta)$ is the product of the displaced parity operator for each mode (A and B),

$$\widehat{\Pi}(\alpha, \beta) = D(\alpha)(-1)^{\widehat{n}_A} D^\dagger(\alpha) D(\beta)(-1)^{\widehat{n}_B} D^\dagger(\beta).$$

This expression shows that the value of the Wigner function at any point $\{\alpha, \beta\}$ in phase space may be measured by first displacing each mode with a complex amplitude (α and β respectively), and then measuring the sum of the parities for the resulting fields. These modes may be in a same cavity and have different frequencies, or may be distributed in two cavities and have the same or different frequencies. It is easy to generalize the procedure discussed before to the direct measurement of the Wigner function corresponding to these modes: after displacing the field in each mode (by different complex amplitudes), one lets the same atom interact dispersively with the two modes, so as to realize the corresponding parity operators. Measurement of the atomic population difference after this interaction leads to the multimode Wigner function (131).

Let us consider a two-mode pure state of the form:

$$|\Psi_{AB}\rangle = a\,|0_A\rangle\,|0_B\rangle + b\,|0_A\rangle\,|1_B\rangle + c\,|1_A\rangle\,|0_B\rangle + d\,|1_A\rangle\,|1_B\rangle\,, \tag{132}$$

where a, b, c, d are arbitrary complex numbers restrained by the normalization condition $\langle\Psi_{AB}\,|\Psi_{AB}\rangle = 1$, and we have restricted ourselves to the state space generated by the possibility of having only the Fock states, $n = 0, 1$ in each mode, A and B.

The quantity of entanglement is defined as [56]

$$E\{\rho_{AB}\} = -2tr\,\{\rho_A \log \rho_A\}\,, \tag{133}$$

where ρ_A is the reduced density operator corresponding to mode A.

For state (132), ρ_A is given by

$$\rho_A = tr_B\{\rho_{AB}\} = \begin{pmatrix} |a|^2 + |b|^2 & ac^* + bd^* \\ a^*c + b^*d & |c|^2 + |d|^2 \end{pmatrix}. \tag{134}$$

The von Newmann entropy corresponding to this density operator may be expressed in terms of the eigenvalues $\lambda_\pm$ of ρ_A:

$$E\{\rho_{AB}\} = -2\{\lambda_+ \log \lambda_+ + \lambda_- \log \lambda_-\}, \tag{135}$$

These eigenvalues are the roots of the equation $\lambda^2 - \lambda + n1 + n2 = 0$, where,

$$n_1 = |a|^2 |c|^2 + |b|^2 |d|^2 - ac^* b^* d - a^* cbd^*, \tag{136}$$

$$n_2 = \left(|a|^2 - |b|^2\right)\left(|d|^2 - |c|^2\right). \tag{137}$$

It will be shown now that n_1 and n_2 can be obtained from four points of the two-mode Wigner function corresponding to the state (132).:

$$W(\alpha, \beta) = \langle \Psi_{AB} | \, \widehat{\Pi}(\alpha, \beta) \, | \Psi_{AB} \rangle \, . \tag{138}$$

It is easy to show that

$$\frac{W(\alpha,0) + W(-\alpha,0)}{2e^{-2|\alpha|^2}} = |a|^2 - |b|^2 + (4|\alpha|^2 - 1)(|c|^2 - |d|^2). \tag{139}$$

Evaluation of this expression for two different values of $|\alpha|$ is enough to determine the population differences $|d|^2 - |c|^2$ and $|a|^2 - |b|^2$, and therefore n_2. Therefore, two pairs of symmetric points lying on different circumferences in the plane $\beta = 0$ determine n_2.

On the other hand,

$$n_1 = \frac{\left[\frac{W(|\alpha|,0) - W(|\alpha| e^{i\pi},0)}{2|\alpha| e^{-2|\alpha|^2}}\right]^2 + \left[\frac{W(|\alpha'| e^{i\frac{\pi}{2}},0) - W(|\alpha'| e^{i\frac{3\pi}{2}},0)}{2|\alpha'| e^{-2|\alpha'|^2}}\right]^2}{4}. \tag{140}$$

More generally, any set of points of the two-mode Wigner function containing the vertices of a losangle located in the plane $\beta = 0$, and centered at $\alpha = 0$, allows one to calculate the eigenvalues of the reduced density matrix for mode A. The only restrictions are that the diagonals of this losangle must be different ($|\alpha'| \neq |\alpha|$), which means that its area must be non-null. Once the eigenvalues of ρ_A are obtained, through this four points, we can fully determine the quantity of entanglement for the proposed system. Obviously the same conditions apply to mode B.

For a three-mode entangled state, it is also possible to relate its entanglement with properties of the Wigner function. In particular, it is possible to show that the value of the Wigner function at the origin of phase space provides a test for the quantum character of a GHZ state [57,58].

X. CONCLUSION

In these lectures, it was shown that techniques used in the field of quantum optics are helpful to discuss the quantum-classical transition, and in particular allow the monitoring of the decoherence process, which is at the heart of the quantum theory of measurement. This does not mean that the problem of the classical limit has been solved. Indeed, one has looked only at the dynamics of linear systems (the field mode coupled to the reservoir oscillators), and therefore we have not discussed the difficult problems related to the classical limit of non-linear systems, where chaotic behavior may play an important role [59]. Furthermore, coherence does not really disappear, and it is still present in entangled states of the cavity field and the rest of the Universe. This fact immediately leads us to the question about the meaning of the wave function of the Universe, and to the seemingly paradoxical application of probability concepts to a Universe which is unique. According to Murray Gell-Man and Jim Hartle, "quantum mechanics is better and more fundamentally understood within the context of quantum cosmology" [60]. Even though fundamental problems related to the classical limit of quantum mechanics and the quantum theory of measurement remain to be solved, I think it is fair to say that quantum optics has helped us to understand and observe an important piece of this puzzle.

ACKNOWLEDGMENTS

This work was partially supported by PRONEX (Programa de Apoio a Núcleos de Excelência), CNPq (Conselho Nacional de Desenvolvimento Científico e Tecnológico), FAPERJ (Fundação de Amaparo à Pesquisa do Estado do Rio de Janeiro), CAPES (Coordenação de Aperfeiçoamento de Pessoal de Ensino Superior), and FUJB (Fundação Universitária José Bonifácio). It is a pleasure to acknowledge the collaboration on the subjects covered by these lecture notes with M. Brune, M. França Santos, S. Haroche, L.G. Lutterbach, J.M. Raimond, and N. Zagury.

---

[1] Letter from Albert Einstein to Max Born in 1954, cited by E. Joos, in *New Techniques and Ideas in Quantum Measurement Theory,* edited by D. M. Greenberger (New York Academy of Science, New York, 1986); see also W. H. Zurek, S. Habib, and J. P. Paz, Phys. Rev. Lett. **70**, 1187 (1993).

[2] E. Schrödinger, Naturwissenschaften **23**, 807 (1935); **23**, 823 (1935); **23**, 844 (1935). English translation by J. D. Trimmer, Proc. Am. Phys. Soc. **124**, 3235 (1980).

[3] J. Von Neumann, *Die Mathematische Grundlagen der Quantenmechanik* (Springer-Verlag, Berlin, 1932); english translation by R. T. Beyer: *Mathematical Foundations of Quantum Mechanics,* (Princeton University Press, Princeton, NJ, 1955)

[4] E. Wigner, in *The Scientist Speculates,* edited by I. J. Good (William Heinemann, London, 1962), p. 284, and also in *Symmetries and Reflections* (Indiana University Press, Bloomington, 1967), p. 171; G. Ludwig in *Werner Heisenberg und die Physik unserer Zeit* (Braunschweig, Friedrich Vieweg und Sohn, 1961). See also E. Wigner, Am. J. of Phys. **31**, No. 1 (1963).

[5] *Quantum Theory and Measurement,* edited by J. A. Wheeler and W. H. Zurek (Princeton Univ. Press, Princeton, 1983); W. Zurek, Phys. Today **44**, No. 10, 36 (1991); R. Omnès, *The Interpretation of Quantum Mechanics* (Princeton University Press, Princeton, NJ, 1994); D. Giulini, E. Joos, C. Kiefer, J. Kupsch, I.-O. Stamatescu, and H. D. Zeh, *Decoherence and the Appearance of a Classical World in Quantum Theory* (Springer, Berlin, 1996).

[6] K. Hepp, Helv. Phys. Acta **45**, 237 (1972); J. S. Bell, Helv. Phys. Acta **48**, 93 (1975).

[7] K. Gottfried, *Quantum Mechanics* (Benjamim, Reading, MA ,1966), Sec. IV.

[8] H. D. Zeh, Found. Phys. **1**, 69 (1970); W. H. Zurek, Phys. Rev. D **24**, 1516 (1981); **26**, 1862 (1982); W. G. Unruh and W. H. Zurek, Phys. Rev. D **40**, 1071 (1989); W. H. Zurek, Phys. Today **44**, No. 10, 36 (1991); B. L. Hu, J. P. Paz, and Y. Zhang, Phys. Rev. D **45**, 2843 (1992).

[9] H. Dekker, Phys. Rev. A **16**, 2116 (1977); A. O Caldeira and A. J. Leggett, Physica (Amsterdam) **121A**, 587 (1983); Phys. Rev. A **31**, 1059 (1985).

[10] E. Joos and H. D. Zeh, Z. Phys. B **59**, 223 (1985); G. J. Milburn and C. A. Holmes, Phys. Rev. Lett. **56**, 2237 (1986); F. Haake and D. Walls, Phys. Rev. A **36**, 730 (1987).

[11] C.H. Bennett, G. Brassard, C. Crépeaus, R. Jozsa, A. Peres, and W.K. Wootters, Phys. Rev. Lett. **70**, 1895 (1993); L. Davidovich, N. Zagury, M. Brune, J. M. Raimond, and S. Haroche, Phys. Rev. A **50**, R895 (1994); D. Bouwmeester, J.-W. Pan, K. Mattle, M. Eible, H. Weinfurter, and A. Zeilinger, Nature **390**, 575 (1997); A. Furusawa, J.L. Sørensen, S.L. Braunstein, C.A. Fuchs, H.J. Kimble, and E.S. Polzik, Science **282**, 706 (1998).

[12] R.G. Hulet and D. Kleppner, Phys. Rev. Lett. **51**, 1430 (1983).

[13] S. Haroche, "Cavity Quantum Electrodynamics", in *Fundamental Systems in Quantum Optics*, J. Dalibard, J. M. Raimond, and J. Zinn-Justin, eds., *Proc. Les Houches Summer School, Session LIII* (Elsevier, Amsterdam, 1992); see also *Cavity Quantum Electrodynamics*, edited by P. Berman (Academic Press, New York, 1994).

[14] R. J. Glauber, Phys. Rev. **131**, 2766-2788, 1963.

[15] W. Pauli, Die allgemeinen Prinzipien des Wellenmechanik, in *Handbuch der Physik*, ed. H. Geiger ad K. Scheel (Springer, Berlin, 1933). English translation: W. Pauli, *General Principles of Quantum Mechanics* (Springer, Berlin, 1980).

[16] U. Leonhardt, *Measuring the Quantum State of Light* (Cambridge University Press, 1997).

[17] Many theoretical and experimental papers have been published on the subject of squeezing. See, for instance, L. A. Lugiato and G. Strini, *Opt. Commun.* **41**, 67 (1982); B. Yurke, *Phys. Rev. A***29**, 408 (1984); M. J. Collet and C. W. Gardiner, *Phys. Rev. A***30**, 1386 (1984); M. J. Collet and D. F. Walls, *Phys. Rev. A***32**, 2887 (1985); R. M. Slusher, L. W. Hollberg, B. Yurke, J. C. Mertz, and J. F. Valley, *Phys. Rev. Lett.* **55**, 2409(1985); H. J. Carmichael, *Phys. Rev. A* **33**, 3262 (1986); R. M. Shelby, M. D. Levenson, S. H. Perlmutter, R. S. DeVoe, and D. F. Walls, *Phys. Rev. Lett.* **57**, 691 (1986); L. A. Wu, H. J. Kimble, J. L. Hall, and H. Wu, *Phys. Rev. Lett.* **57**, 2520 (1986); M. D. Reid and D. F. Walls, *Phys. Rev. A* **33**, 4465 (1986); M. D. Reid and D. F. Walls, *Phys. Rev. A* **34**, 4929 (1986); D. A. Holm, M. Sargent III, and B. A. Capron, *Opt. Lett.* **11**, 443 (1986); M. W. Maeda, P. Kumar, and J. H. Shapiro, *Opt. Lett.* **12**, 161 (1987); S. Reynaud, C. Fabre, and E. Giacobino, *J. Opt. Soc. Am. B***4**, 1520 (1987); A. Heidmann, R. Horowicz, S. Reynaud, E. Giacobino, C. Fabre, and G. Camy, *Phys. Rev. Lett.* **59**, 2555 (1987); M. G. Raizen, L. Orozco, M Xiao, T. L. Boyd, and H. J. Kimble, *Phys. Rev. Lett.* **59**, 198 (1987); L. A. Orozco, M. G. Raizen, M. Xiao, R. J. Brecha, and H. J. Kimble, *J. Opt. Soc. Am.*

4, 1490 (1987); S. F. Pereira, M. Xiao, H. J. Kimble, and J. L. Hall, *Phys. Rev. A* **38**, 4931 (1988); P. D. Drummond and M. D. Reid, *Phys. Rev. A***37**, 1806 (1988); F. Castelli, L. A. Lugiato, and M. Vadacchino, *Nuovo Cimento* **10**, 183 (1988); M. D. Reid, *Phys. Rev. A* **37**, 4792 (1988); S. Reynaud and A. Heidmann, *Opt. Commun.* **71**, 209 (1989); J. Mertz, T. Debuisschert, A. Heidmann, C. Fabre, and E. Giacobino, *Opt. Lett.* **16**, 1234 (1991); see also the special issues Journal of the Optical Society of America B**4**, 1987; Journal of Modern Optics **34**, 1987; and Applied Physics B **55**, 1992.

[18] R. Loudon and P. Knight, J. Mod. Opt. **34**, 709 (1987).

[19] H. P. Yuen and J. H. Shapiro, IEEE Trans. IT **26**, 78 (1980); C. M. Caves, Phys. Rev. D **23**, 1693 (1981); B. L. Schumaker, Opt. Lett. **9**, 189 (1984).

[20] J. Bertrand and P. Bertrand, Found. Phys. **17**, 397 (1987).

[21] J. Radon, *Berichte über die Verhandlungen der Königlich-Sächsischen Gesellschaft der Wissenschaften zu Leipzig, Mathematisch-Physiche Klass* **69**, 262 (1917).

[22] E. Wigner, Phys. Rev. **40**, 749 (1932).

[23] K. E. Cahill and R.J. Glauber, Phys. Rev. **177**, 1857 (1969); *ibid* **177**, 1882 (1969).

[24] M. Hillery, R. F. O'Connell, M. O. Scully, and E. P. Wigner, Phys. Rep. **106**, 121 (1984).

[25] R.L. Hudson, Rep. Math. Phys. **6**, 249 (1974).

[26] J. E. Moyal, Proc. Cambridge Phil. Soc. **45**, 99 (1949).

[27] See, for instance, H. M. Nussenzveig, *Introduction to Quantum Optics* (Gordon and Breach, N.Y., 1973); C. W. Gardiner, *Quantum Noise* (Springer, Berlin, 1991).

[28] K. Vogel and H. Risken, Phys. Rev. A **40**, 2847 (1989).

[29] D.T. Smithey, M. Beck, M. G. Raymer and A. Faridani, Phys. Rev. Lett. **70**, 1244 (1993).

[30] G. Breitenbach, T. Müller, S. F. Pereira, J.-Ph. Poizat, S. Schiller and J. Mlynek, J. Opt. Soc. Am. B **12**, 2304 (1995).

[31] T. J. Dunn, I. A. Walmsley, and S. Mukamel, Phys. Rev. Lett. **74**, 884 (1995).

[32] D. Leibfried, D. M. Meekhof, B. E. King, C. Monroe, W. M. Itano and D. J. Wineland, Phys. Rev. Lett. **77**, 4281 (1996); see also Physics Today **51**, no. 4, 22 (1998).

[33] M. Brune, S. Haroche, J. M. Raimond, L. Davidovich, and N. Zagury, Phys. Rev. A **45**, 5193 (1992).

[34] E. T. Jaynes and F. W. Cummings, Proc. IEEE **51**, 89 (1963).

[35] R. P. Feynman, F. L. Vernon, Jr., and R. W. Hellwarth, J. Appl. Phys. **28**, 49 (1957).

[36] G. Grynberg, J. Dupont-Roc, and C. Cohen-Tannoudji, *Atom-Photon Interactions: Basic Processes and Applications* (Wiley, N.Y., 1992).

[37] R. G. Hulet and D. Kleppner, Phys. Rev. Lett. **51**, 1430 (1983); A. Nussenzveig, J. Hare, A. M. Steinberg, L. Moi, M. Gross, and S. Haroche, Euro. Phys. Lett. **14**, 755 (1991).

[38] M. Brune, P. Nussenzveig, F. Schmidt-Kaler, F. Bernardot, A. Maali, J. M. Raimond, and S. Haroche, Phys. Rev. Lett. **76**, 1800 (1996).

[39] N. F. Ramsey, *Molecular Beams* (Oxford Univ. Press, N. Y., 1985).

[40] A. Einstein, B. Podolski, and N. Rosen, Phys. Rev. **47**, 777 (1935).

[41] J. S. Bell, Physics (Long Island City, N. Y.) **1**, 195 (1964).

[42] S. J. Freedman and J. S. Clauser, Phys. Rev. Lett. **28**, 938 (1972); A. Aspect, J. Dalibard, and G. Roger, Phys. Rev. Lett. **49**, 1804 (1982).

[43] M. Brune, E. Hagley, J. Dreyer, X. Maître, A. Maali, C. Wunderlich, J. M. Raimond, and S. Haroche, Phys. Rev. Lett. **77**, 4887 (1996).

[44] L. Davidovich and V. M. Kenkre, to be published.

[45] L. G. Lutterbach and L. Davidovich, Phys. Rev. Lett. **78**, 2547 (1997); *ibid* Optics Express **3**, 147 (1998).

[46] L. Davidovich, M. Orszag, and N. Zagury, Phys. Rev. A **57**, 2544 (1998).

[47] L. Davidovich, A. Maali, M. Brune, J. M. Raimond and S. Haroche, Phys. Rev. Lett. **71**, 2360 (1993); L. Davidovich, M. Brune, J. M. Raimond and S. Haroche, Phys. Rev. A **53**, 1295 (1996).

[48] X. Maître, E. Hagley, G. Nogues, C. Wunderlich, P. Goy, M. Brune, J. M. Raimond and S. Haroche, Phys. Rev. Lett. **79**, 769 (1997).

[49] G. Nogues, A. Rauschenbeutel, S. Osnaghi, P. Bertet, M. Brune, J. M. Raimond, S. Haroche, L. G. Lutterbach, and L. Davidovich, to be published in Phys. Rev. A (2000).

[50] G. Nogues, A. Rauschenbeutel, S. Osnaghi, M. Brune, J. M. Raimond, and S. Haroche, Nature **400**, 239 (1999).

[51] E. Hagley, X. Maître, G. Nogues, C. Wunderlich, M. Brune, J. M. Raimond, and S. Haroche, Phys. Rev. Lett. **79**, 1 (1997).

[52] D. M. Greenberger, M. A. Horne and A. Zeilinger, Am. J. Phys. **58**, 1131 (1990); D. Bouwmeester *et al.*, Phys. Rev. Lett. **82**, 1345 (1999).

[53] A. Rauschenbeutel, G. Nogues, S. Osnaghi, P. Bertet, M. Brune, J.-M. Raimond, and S. Haroche, Science **288**, 2024 (2000).

[54] K. Banaszek and K. Wódkiewicz, Phys. Rev. Lett. **82**, 2009 (1999).

[55] M. França Santos and L. Davidovich, submitted to publication.

[56] C.H. Bennett, H.J. Bernstein, S. Popescu, and B. Schumacher, Phys. Rev. A **53**, 2046 (1996).

[57] D.M. Greenberger, M.A. Horne, and A. Zeilinger, in *Bell's Theorem and the Conception of the Universe*, edited by M. Kafatos (Kluver Academic, Dordrecht, 1989); D.M. Greenberger, M.A. Horne, A. Shimony and A. Zeilinger, Am. J. Phys.

58, 1131 (1990); David Mermin, Phys. Today, **43**, 9 (1990).
[58] L.G. Lutterbach, M. França Santos, and L. Davidovich, submitted to publication.
[59] W.H. Zurek and J.P. Paz, Phys. Rev. Lett. **72**, 2508 (1994); S. Habib, K. Shizume, and W. H. Zurek, Phys. Rev. Lett. **80**, 4361 (1998).
[60] M. Gell-Mann and J. B. Hartle, "Quantum mechanics in the light of quantum cosmology", in *Complexity, Entropy, and the Physics of Information*, edited by W. H. Zurek, p. 425 (Addison-Weslwy, Reading, 1990).